

THESIS ON POWER ENGINEERING, ELECTRICAL ENGINEERING,  
MINING ENGINEERING D25

**Development and Research of the Traction  
Asynchronous Multimotor Drive**

**Vitaly Boyko**

TUT  
PRESS

Department of Electrical Drives and Power Electronics  
Faculty of Power Engineering  
TALLINN UNIVERSITY OF TECHNOLOGY

Dissertation is accepted for the commencement of the degree of Doctor of Science in Natural and Exact Sciences on April, 2008

Supervisor: Prof Juhan Laugis, Faculty of Power Engineering

Opponents:

Professor Ryszard Strzelecki, DSc., PhD, Gdynia Maritime University, Poland.

Professor Ivars Rankis, Dr Sc. eng., Riga Technical University, Latvia

Associate professor Alexander Vodovozov, PhD., Vologda Technical University, Russia

Commencement: May, 2008

Declaration: Hereby I declare that this doctoral thesis, my original and independent investigation and achievement, submitted for the doctoral degree at Tallinn University of Technology has not been submitted for any degree or examination in any other institution.

Vitali Boiko, .....

Copyright Vitali Boiko 2008

ISSN

ISBN

# TABLE OF CONTENT

SYMBOLS .....	10
ABBREVIATIONS .....	14
INTRODUCTION .....	16
1 STATE-OF-THE-ART ANALYSIS AND DEVELOPMENT PROSPECTIVE OF TAMD .....	18
1.1 AC motor drives of trams and metro (Siemens) .....	18
1.2 Motor drives of E4 Series electrical trains.....	19
1.3 TAMD classification .....	20
1.4 Conclusions .....	21
2 STRUCTURAL-POWER SYNTHESIS OF TAMD .....	22
2.1 Structure analysis and configuration basis of TAMD.....	22
2.1.1 Selection of configuration .....	22
2.1.2 Drive model development .....	24
2.1.3 Structure forming of KT-4 tram traction system .....	25
2.2 Comparative analysis and TAMD simulation tool selection .....	29
2.2.1 Classification.....	29
2.2.2 Code Composer Studio 2.0.....	29
2.2.3 Microsoft Visual C++ 6.0.....	29
2.2.4 Matlab 6 .....	29
2.2.5 PSCAD.....	30
2.2.6 Comparative analysis of the simulation tools.....	30
2.2.7 Selection of the simulation tool.....	30
2.3 Development and identification of the induction motor equivalent circuit.....	31
2.3.1 Equivalent circuit .....	31
2.3.2 Experimental search of the equivalent circuit parameters .....	31
2.3.3 Determination of stator winding resistance .....	32
2.3.4 Short circuit experiment .....	32
2.3.5 Resistance calculation .....	33
2.3.6 Open circuit experiment .....	34
2.3.7 Theoretical calculations.....	36

2.4	Simulation and research of the TAMD power unit.....	37
2.4.1	Simulation of the induction motor .....	37
2.4.2	Simulation of the inverter.....	38
2.4.3	Simulation of the drive mechanical unit.....	38
2.5	Development of the calculation method of the traction motor power .....	40
2.5.1	Calculation method .....	40
2.5.2	Calculation examples .....	42
2.5.3	Motor selection for Estonia.....	43
2.6	Traction calculation of the tram motor drive .....	45
2.6.1	Problem definition.....	45
2.6.2	Development of the motor mode calculation method .....	46
2.6.3	Development of the calculation method for the traction motor generator modes .....	47
2.6.4	Development of the method for the braking unit calculation.....	48
2.7	Conclusions .....	48
3	DEVELOPMENT OF THE DESIGN METHOD FOR THE TAMD FREQUENCY CONVERTERS .....	50
3.1	Analysis of the methods and tools for the TAMD frequency converter control .....	50
3.1.1	Problem statement.....	50
3.1.2	Selection of the control principle for the traction drive .....	51
3.1.3	Problem statement of vector control in parallel coupled traction induction motors .....	52
3.1.4	Model of Multimotor Drive with Frequency Converter.....	58
3.1.5	Analysis of the Frequency Converter Operation in the Multimotor Drive.. ..	61
3.2	Development of the circuit design method and power switch selection for the TAMD converter .....	65
3.2.1	Selection of controlled switch types.....	65
3.2.2	Method for IGBT calculation.....	68
3.2.3	Algorithm Selection for the Traction Converter Switch Control .....	69
3.3	Design of the input LC filter for the power converter .....	71
3.3.1	Mathematical model of the input LC filter.....	71

3.3.2	Variants of input filters.....	74
3.3.3	Calculation of the input filter for N inverters .....	74
3.3.4	Calculation of the input filter for two inverters .....	76
3.3.5	Calculation of the input filter for four inverters .....	76
3.4	Conclusions .....	77
4	COMPUTER SIMULATION AND EXPERIMENTAL RESEARCH OF MOTOR DRIVE COMPONENTS.....	78
4.1	Computer simulation .....	78
4.1.1	Control system model.....	78
4.1.2	Simulated processes and result analysis .....	80
4.2	Development of the tamd control system elements .....	80
4.2.1	Development of the control method for induction motor field weakening.. .....	80
4.2.2	Development of the speed measuring device for the induction motor .....	87
4.2.3	Analysis of solutions to the TAMD electromagnetic compatibility problem.....	90
4.2.4	Development of current measuring tools for the frequency converters...94	
4.3	Conclusions .....	97
5	SUMMARY .....	99
6	REFERENCES.....	101
	ABSTRACT .....	106
	LÜHIKOKKUVÕTE (ANNOTATSIOON).....	107
	PUBLICATION.....	108
	LISA / ANNEX 1 .....	111
	ELULOOKIRJELDUS .....	111
	CURRICULUM VITAE.....	114

## OBJECTIVES OF THE THESIS

**Subject area:** traction motor drive of municipal electric transport, predominantly trams and electric trains. The thesis is devoted to the solution of scientific problems related to improving and creation of multimotor ac drives leading to an increase of the transport productivity and reliability and to improve its technical, economic, and ergonomic odds.

**Thematic topicality** is explained by the practical needs of the country in effective, ergonomic, and safe transport means. Research is based on the novel theoretical results and progressive technologies in the field of driving engineering and power electronics, developed in the last years in the European Union and particularly in Estonia. The thematic choice is determined by the national market demands and high priority problems proposed during the decennial collaboration of TTU and TTTO.

**The goal of the thesis** is to develop and study the novel hardware, software, and technological tools in the field of traction asynchronous multimotor drive (TAMD).

### **The main problems of the thesis are:**

1. State analysis and development perspectives of TAMD
2. Development and approbation of the novel method of structural and power TAMD synthesis
3. Building the method of the TAMD frequency converter design
4. Development of the mathematical model and experimental research of the main drive components.

### **The main results of the thesis are:**

1. Analyses of the traction drive power circuits and classification of the driving tools in the field.
2. Engineering and economic basics of the needs for development and research of the novel motor drive system using the solutions proposed earlier in the Department of Electrical Drives and Power Electronics.
3. Analysis, comparison, and regimentation of the known and prospective principal decisions in the TAMD configuration scope.
4. Solution of topology optimization problems and composition of traction ac drives, including the choice of motor and converter types, control methods, and element base.

5. Comparative analysis and selection of the TAMD simulation tools including the grounding of the required software.
6. Development and identification of the induction motor equivalent circuit for the multimotor traction system, including comparative analysis of the methods to obtain equivalent circuit parameters.
7. Development and test of the TAMD calculation and motor selection methods including the grounding of the possible replacement of the entity dc motors by the ac ones.
8. Method of the calculation of motor drive traction including the motor and generator modes, and inverter braking resistor.
9. Comparative analysis of the TAMD frequency converter control structures including the proof of the vector control requirement.
10. Development of the vector control algorithms for the group of parallel-connected induction traction motors.
11. Comparative analysis of the suggested vector control algorithms including the selection of an optimum one.
12. Design method of the input LC filter for the power converter and test results of calculation algorithms for two, four, and N inverters.
13. Computer model of the motor drive control system built to study different modes of operation.
14. Technology and results of computer research in the capacitor charge of the dc link supplied by the single-phase and three-phase mains, including search for optimum conditions for a single and two motor running from different supply.
15. Novel approach to the induction motor control with the field weakening taking into account various possibilities of such adjustment.
16. Development of a formula to calculate the required motor flux using its rated value and speed, including the analysis of the product area.
17. Novel method of the dynamic field weakening, which enables flexible tuning of the motor flux to obtain its maximum value even under the reduced voltage, including the analysis of its product area.
18. Circuit of the series connection for the two field weakening units, which provides the required unit operation under the rated voltage level thus giving rise to the drive stability.
19. Novel device for the induction motor speed measurement.
20. Novel device for the frequency converter current measurement, which excludes the main sources of electromagnetic emission.

21. Method of the DSP usage to obtain the required system current quality, including the practical results of its applying.

**Scientific novelty of the thesis:**

1. Original topology and composition of the traction multimotor drive.
2. Computer model of the drive control system intended for study of variable modes of operation.
3. Algorithm of vector control for the group of parallel-connected induction traction motors.
4. New approach to the induction motor control by the field weakening with different control possibilities.
5. Method of the TAMD induction motor calculation and selection.
6. Method of the drive traction calculation including motor and generator mode calculation as well as the inverter braking unit calculation.
7. Design method for the input LC filter of the power converter, including the input filter calculation for two, four, and N inverters.
8. Technology and computer research results of the dc unit capacitor charging modes for the single-phase and three-phase supply mains suitable for the optimum running conditions of the single and two motors supplied by different sources.
9. Formula for the calculation of the required motor flow using the rated motor value and speed including the analysis of the product area.
10. Method of the dynamic field weakening suitable for the safe motor flow tuning to obtain a maximum possible flow even under the reduced voltage, including the analysis of its product area.
11. Circuit of the two field-weakening unit's series connection suitable for the static field weakening unit operation under the rated voltage level, which leads to improvements in the drive stability.
12. Device for measuring induction motor speed and the method for optimum measuring the speed of the rotor rotation.
13. Device for measuring the phase current for frequency converters with minimum influence of electromagnetic emission upon the result data.
14. Method of the DSP usage to obtain the desired system current measuring quality as well as the practical results in the use of the suggested solution.
15. Induction motor equivalent circuit suitable for the multimotor traction system.

### **Practical significance of the thesis:**

1. Technical and economic confirmation of the research in the field served as the basis of the new drive system development.
2. Solution of the problem of the traction ac drive optimal topology and composition contributed to the choice of motor and converter types, control methods, and element base.
3. Comparative analyses and TAMD simulation tools selection allowed the project to be provided with the required software.
4. The developed equivalent circuit of the induction motor promoted the parameter identification of the multimotor traction system.
5. Method of the TAMD induction motor calculation and selection provided a basis to move the rationality of replacement of the existing dc motors by the ac motors.
6. Drive traction calculation method was established as a basis of the motor and generator modes calculations as well as the inverter braking unit calculation.
7. Development of the vector control algorithms for the group of parallel-connected induction traction motors contributed to finding optimum control algorithms for the desired system.
8. Design method of the power converter input LC filter was established as a basis of input filter calculations for two, four, and N inverters.
9. Computer model of the drive control system allowed for searching various modes of the drive operation.
10. Research into the dc link capacitor charging technology under the single-phase and three-phase supply enabled to find the optimum running conditions for the single and two motors supplied by different sources.
11. Novel method of the dynamic field weakening allowed the motor flow safe tuning to obtain the maximum possible value even under the reduced voltage.
12. Circuit of the series connection of the two field-weakening units provided the static field-weakening module operation under the rated voltage level thus improving the drive stability.
13. Induction motor speed measuring device was established as a basis of the encoder signal interpreting method.
14. Novel device for measuring frequency converter current allowed different hardware and software to be used to suppress the noise resulting from the converter electromagnetic emission.

## SYMBOLS

$a$	tram acceleration	$f_k$	dependent constant of the braking resistor
$\alpha$	overcoming slope angle	$f_{tr}$	rolling friction factor, mm (steel wheels, flat rail)
$A, S$	cross-section	$F_w, F_b$	aerodynamic resistance force
$b$	friction factor between wheel ledge and rails (conical rim wheels)	$F_{дин}$	tram inertia force
$B$	tram width	$F_k$	wheel propulsive force
$CF$	input filter inductance and capacity	$F_k$	resulting counter-motive force
$C_n$	snubber capacity	$f_k$	commutation frequency
$C_{ax}$	input capacitance	$F_{под}$	rise resistance force
$dcCur$	dc link current value	$F_{comp}$	tram resulting counter-motive force
$dcCurrentAV$	dc link average current	$F_{rp}$	wheel rolling resistance force
$dcVltg$	dc link voltage	$g$	gravity acceleration
$d_r$	wheel diameter	$H$	tram height
$\Delta t$	time interval while current flows from inverter to source	$H$	rotor equivalent constant
$\Delta U_C$	possible overvoltage on the capacitor	$\eta_{и}$	inverter efficiency
$f$	supply voltage frequency	$\eta_p$	gear efficiency
$F$	rotor equivalent friction factor	$\eta_{тэд}$	traction motor efficiency
$f_{cp}$	cutoff frequency	$i, u$	gear ratio
$f_0$	motor supply voltage frequency	$I_1, I_2$	motor current
$f_{0H}$	supply voltage rated frequency	$I_a, I_b, I_c$	phase currents of three-phase mains
$F_f$	slope resistance	$I_{aInv}, I_{bInv}, I_{cInv}$	inverter output currents curves (instant values)
		$I_{aInvRM}$	inverter output current effective

S	value	$L_s$	stator inductance
$I_d$	dc link current	$I_s$	stator current
$I_{d, ids}$	d axis stator current	$I_\mu$	magnetization current
$i'_{dr}$	d axis rotor current	$L_{rp}$	inductor inductance
$I_n$	rated current	$\lambda_m$	torque ratio
$I_q, i_{qs}$	q axis stator current	$\mu$	modulation factor
$i'_{qr}$	q axis rotor current	m	mass
$i_{s\_abc}$	phase a, b, c stator currents	$M_{bmax}$	maximum braking torque
J	rotor equivalent moment of inertia	$M_{load}$	load torque
$J_{ekv}$	equivalent moment of inertia	$m_n$	pulse number of the rectified voltage per supply voltage period
$J_{ges}$	tram motor equivalent moment of inertia	$n_1$	motor maximum rounds per minute
k	generator mode derating	$n_2, n_n$	motor rated rounds per minute
kf	wheel-rail coupling factor	$N_m$	number of parallel-connected motors
$k_s$	factor of front area increase caused by the converter and pantograph accommodation on the tram roof	$n_s$	synchronous rotational speed
L	inductance	$n_{nom}$	rated rotational frequency
$I_0$	no-load current	p	pair pole number
LF	input filter inductance and capacity	$P_0$	no-load power
$I_{fe}$	steel losses current	$P_{bmax}$	maximum braking energy
$L_h$	mutual inductance	$P_{electr}$	maximum electric braking energy including motor inner losses
Ik	short circuit current	$P_{F,comp}$	counter-forces power, kW
$L'_{lr}$	rotor reluctance	$\Phi_{hir}^*$	required motor flow
$L_s$	stator reluctance	$\Phi_{hir}, \varphi$	motor flow

$P_k$	short-circuit power	$T_{m2}$	expected load torque
$P_{n,motor}$	rated motor power	$t_r$	rotor time constant
$P_{dmm}$	dynamic power	$T_s$	static load torque
$\rho$	air density	$t_z$	maximum cycle time, s
$R_{fe}$	steel losses resistance	$U$	rms supply voltage value
$R_g$	grounding resistance	$U_0$	no-load voltage
$R_l$	inductor active resistance	$U_{\alpha}$	$\alpha$ axis voltage
$R_n$	snubber resistance	$U_{\beta}$	$\beta$ axis voltage
$R_r', R_r$	rotor active resistance	$U_{dc}$	dc supply voltage
$R_s$	supply line resistance	$U_k$	short circuit voltage
$R_s', R_s$	stator active resistance	$U_n$	rated voltage
$R_{thjc}$	transient resistance between transistor and diode crystals and case under the definite cooling conditions, Ohm	$U_{ri}$	required amplitude of the output voltage ripple
$s$	slip	$v$	motor linear velocity
$S_a, S_b, S_c$	inverter control signals	$V_a, V_b, V_c$	phase voltages of three-phase mains
$s_k$	critical slip	$V_{cesat}$	threshold voltage of the transistor saturation
$s_{nom}$	rated slip	$V_{dr}$	d axis rotor voltage
$t_b$	relative braking time	$V_{ds}$	d axis stator voltage
$T_{case}$	case temperature	$V_{qr}$	q axis rotor voltage
$T_e$	electromagnetic torque	$V_{qs}$	d axis stator voltage
$T_e^*$	required motor torque	$V_{source}$	ripple voltage source
$T_{\theta}, \theta$	rotor electrical angle		corresponding motor speed (1-first, 2-second) per-unit, where 1 is the synchronous rotational speed
$T_{j(max)}$	junction maximum temperature	$w_1, w_2$	
$T_m$	motor load torque	$w_{m2}, v$	tram linear velocity

$\omega_c$	supply voltage frequency	angular	$\varphi'_{qr}$	q and d axes rotor magnetic fluxes
$X_h$	magnetization impedance	circuit	$\varphi_{qs}$	q and d axes stator magnetic fluxes
$X_r, L_r$	rotor full reluctances		$\omega_{mech}, \omega, \omega_m$	mechanical rotor speed
$X_s, L_s$	stator full reluctances			
$\gamma$	inertia factor of rotational parts		$a_{KT-4}$	deceleration provided by the regular dc motor
$\Delta P_m$	mechanical losses		$a_{\text{pe6}}$	legitimate deceleration
$\theta_m$	rotor angular position		$P_{KT-4}$	rated power of KT – 4 tram regular traction motor
$\mu$	rolling bearings friction factor (roller bearings)		$C_{w,k}$	aerodynamic resistance factor
$\varphi'_{dr}$	q and d axes magnetic fluxes		T	motor actual torque
$\varphi_{ds}$	q and d axes stator magnetic fluxes		$T_H$	motor rated torque

## ABBREVIATIONS

4QS	four-quadrant controller	IEC	International Electrotechnical Commission
Ab	discharger	IGBT	Insulated Gate Bipolar Transistor
AC	alternating current	IGCT	Integrated commutated thyristor gate
alu	arithmetic logical unit	Iv	inverter
boot rom	loading memory area	IW	current transformer
CAN	connection area net protocol	IWR	pulse inverter
CSTBT	Carrier Stored Trench Gate Bipolar Transistor	LC	inductive-capacitive
Cv	input controller	PWM	pulse-width modulation
CZ	intermediate link capacitors	Quadrature CLK	fourfold processor frequency
DC	direct current	ram	random access memory
DIN	German industrial standard	RC	active-capacitive
DIR	rotational direction signal	S	pantograph
DPU	traction converter	SiC	silicon carbide
DTC	direct torque control	StW	motor carriage
E	earth device	SW	voltage transformer
EMTDC	ElectroMagnetic Transients DC	Tr	traction transformer for two motor carriages
G	grounding	ADC	analog-to-digital converter
GTO	Gate Turn-Off Thyristor	AED	asynchronous electric drive
Gui	graphical user interface	GOST	Russia state standard
HA	auxiliary equipment	EC	European Community
HBU	supply converter of auxiliary equipment	DPB	dc pulse breakover
HS	main switch	E	efficiency

M	traction motor	TTU	Tallinn Technical University
PI	proportional-integral	TM	traction motor
TAMD	traction asynchronous multimotor drive	EMI	electromagnetic interference
TVC	thyristor voltage converter	EMS	electromechanical system
TTU	Tallinn Tram-Trolleybus Union		

## INTRODUCTION

The goal of the thesis was to develop a new traction asynchronous multimotor drive (TAMD) for the railway transport based on the induction squirrel-cage rotor motors. A new drive concept will enable a significant reduction of the engineering maintenance expenses. The use of the algorithms for drive vector control will increase the motor running torques and will result in smooth motion. Introduction of two independent inverters will result in continued tram moving in the case of disrepair of one of its motoring trolleys. The drive concept developed with light revision may be used in any type of rail transport. In Estonia, this drive may be employed in Estonian electrical railway and in the design of national tram models.

New engineering solutions in the field of railway transport are not frequent. These concern mainly actual equipment and technical unit renovation. Each improvement bears more or less fruits uncouthness.

Introduction of a squirrel-cage rotor induction motor may be called a revolutionary transformation in the field. An idea of the dc motor replacement by an induction motor appeared long ago thanks to its high reliability and economy, though the problem was in the three-phase supply and motor adjustment.

Next generation rolling stock on the must help to strengthen railway positions in their concurrent competition with other means of transportation. For this purpose, it has to be economical and attractive for the clients. The rolling stock economy is defined not only by the capital investments into its creation but also by the common life cycle expenditures that affect the reliability and full efficiency. High attractiveness among the passengers is reached by the acceptable tariffs and high train velocity, supported by the necessary comfort level.

Advancements in the microprocessor technique contributed to the design of intelligent and accurate traction ac motor control systems. Such systems guarantee high capacity of work, reliability, reduced maintenance expenses, and economy that are of substantial importance in today's terms. As the German specialists found, using equipment of carriages by the asynchronous drive about 10-15% economy of electrical energy is gained. Such energy consumption of railway transport will save the capitals of many companies involved in the transit by rail freightage.

Control systems of the ac traction drives have to provide full motor controllability, implementation of complex control algorithms as well as the required performance. In addition to the requirements that are common also

for other control systems of industrial drives, the traction drive has some specific needs, specifically relevant to wheel-rail optimal coupling, smooth running and braking, and common supply of a group of parallel-connected motors by the single inverter.

Two types of electric railway transport are typical of Estonia: trams and local electric trains. Tram service is an integral part of Tallinn's city traffic infrastructure. On August 24, 2008, Tallinn trams celebrated their 120th anniversary. Tallinn is the only Estonian city that provides this kind of passenger transport. Historically, tram were purchased from Czech Republic from 1973. The last KT-4 model tram was obtained in 1990. In the next years, TTTU made no investments to new trams due to the municipal budget problems. Today, the main attention is paid to the capital repairs and modernization of the rolling stock to enlarge their resource from 19 (stated by the manufacturer) to 25–30 years [ИЕР06].

In 1998, the collaboration in the field of rolling stock modernization started between TTTU and TTU Department of Electrical Drives and Power Electronics, which has been developing successfully. In 2000, the Department of Electrical Drives and Power Electronics designed a PWM converter to replace the relay control circuit of the traction motors and their starting rheostats in the KT-4 tram. This converter has been built on IGBTs with a microprocessor control system. Replacement of the starting rheostat circuits by the PWM converters allows significant drop in the energy consumption of the railway transport thanks to the rise in the efficiency of the traction drive and energy turnover during the regenerative braking. In addition, TTU has close collaboration with Elektriraudtee AS Company providing some joint projects in the field. Particularly, they search modernization possibilities of the rolling stock, motor-generator auxiliary converter replacement by the static voltage converter, improvements in train's information system, etc.

**Conclusions:** The introduction presents the goal of the thesis and shows its scientific topicality. It gives a historic background of the electric railway transport development. Main scientific discoveries are described that led to spasmodic development in traction electric transport. The invention of self-closed switches and rapid developments in the microprocessor technique contributed to the novel approach to the traction drive. Data concerning Estonian electric railway transport are given. Collaboration directions of TTU and TTTU are provided targeted to starting up the modernized KT4 tram equipped by the transistor traction dc electric drive. Other examples of TTU collaboration with Estonian railway are also represented.

# 1 STATE-OF-THE-ART ANALYSIS AND DEVELOPMENT PROSPECTIVE OF TAMD

Traction drives of all types of rail transport are based on the same concept and are controlled by similar algorithms though their construction depends on particular maintenance conditions. In the first place, it concerns the types of current and supply voltage. The traction converter configuration depends on these parameters. 600-1500 VDC is used for trams and metro supply, 1500-3000 V - for local trains, 3 kVDC and 15-25 kVAC - for long-distance trains.

## 1.1 AC motor drives of trams and metro (Siemens)

The power circuit suggested by Siemens Corporation is shown in Fig. 1.1. It is used for the tram carriages supply from the dc contact net of rated voltage 750 V.

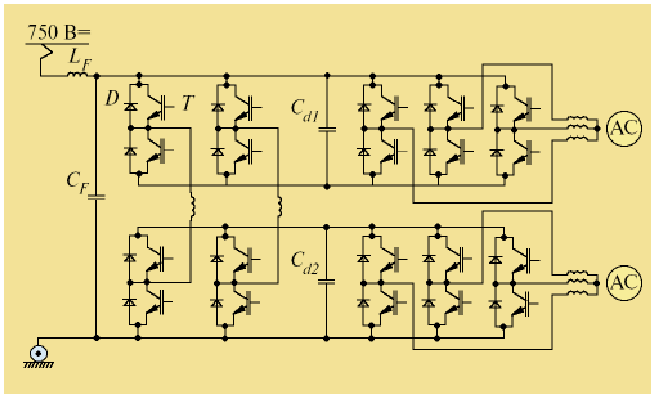


Fig. 1.1 Motor drive of the rolling stock supplied by 750 VDC

$L_F$ ,  $C_F$  — inductance and capacitance of the input filter;  
 $T$  — IGBT;  $D$  — counter-parallel diode;  $C_{d1}$ ,  $C_{d2}$  — capacitor batteries of the intermediate link; AC — induction traction motor

Due to the 1200 V transistor voltage restriction of the early IGBT-technology, dc pulse breakers (DPB) as well as the three-node converters can be used. Figure 1.1 shows this converter circuit having the input pulse breaker for the R1 tram carriages from Frankfurt-on-Main. Its maintenance takes into account the voltage sum of intermediate loops, which exceeds the

contact net voltage. These converters are equipped with the passive circuits of the voltage limiters.

Since the appearance of the first 1700 V IGBTs, the circuit presented in Fig. 1.2 has been used for the supply from the 750 V contact net. When the 6,5 kV locked thyristors appeared, a new converter structure became feasible, with the pulse inverter connected directly to the contact net dc voltage equal to 3 kV of an equivalent analog circuit. Firstly, this circuit has been used to supply electric trains of Desiro Family developed for the Slovenia railways as well as to the trains of the municipal railway CPTM in Brasilia [Bak02].

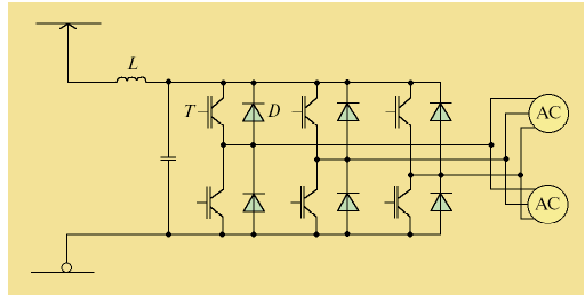


*Fig. 1.2 Traction inverter for the direct supply from the dc contact net*

*Position designations are the same as in Fig. 1.1*

Other examples of multimotor drives are included into the full thesis version.

## **1.2 Motor drives of E4 Series electrical trains**

The train motor carriages are presented by the two electrical groups, each of which has the single pantograph, one traction transformer, and four converter units. Figure 1.3 shows the circuit of the motor carriage traction chain, under which the traction transformer is placed. To adjust the voltage and frequency, the traction drive system uses converters built on IGBTs and tested in the F2 Series train.

The novel technology allowed the reduction of the noise level of the main transformer and its losses caused by the higher harmonics, thus provided more spared temperature mode of the traction motor windings.

The circuit uses the transistor-diode groups of three different types: 3300 V and 1200 A, 3300 V and 600 A, 2500 V and 1000 A. The intermediate link voltage is 2600 VDC.

Rotational frequency and rotational torque of the three-phase squirrel-cage rotor induction motor connected in parallel to the converter are adjusted by PWM depending on the coupling force of the traction and braking modes. As the technical characteristics show, the motor rated power is 10 kW higher than E1 Series train motors have.

The circuit uses the capacitors in the intermediate dc link converter preliminarily charged by the separate transformer winding connected to the specific bridge rectifier. Thus, the circuit has no oscillations when the converter obtains the contact net voltage and the charging resistor with its switching devices is not required here [SAT98].

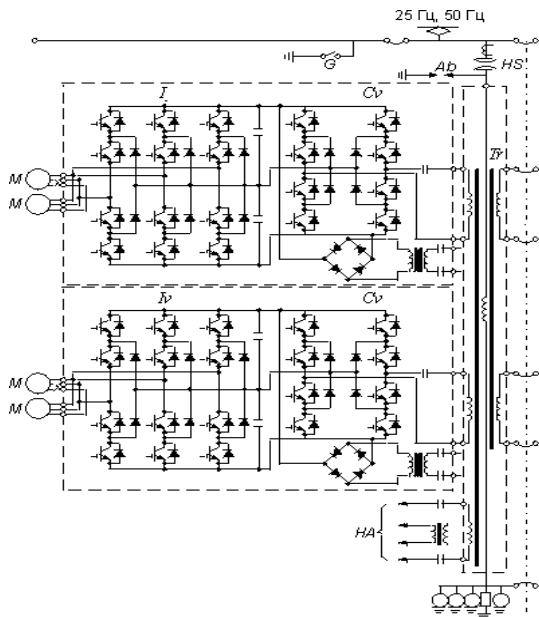


Fig. 1.3 Principal circuit of the motor carriage traction link with a transformer: G - grounding; Ab - discharger; HS - main switch; Tr - traction transformer for two motor carriages; Cv - input controller; Iv - inverter; M - traction motors; HA - auxiliary equipment

### 1.3 TAMD classification

An overwhelming majority of the railway transport traction drives have the multimotor configuration. The specific feature of the rolling stock traction drive is the identical load of all motors participating in the traction generation. In ideal conditions, the traction motors may be viewed as the single motor having the equivalent power, which is equal to the sum of all carriage powers. Nevertheless, in reality drive control is more complex

because of differences in wheel diameters, motor parameters, and wheel-rail coupling forces. In this section, classification of traction drives is not discussed, but the specific features are described.

TAMD may be classified using different indications. First, the number of motors supplied by the single inverter is concerned. The most widespread variants involve one, two, and four motors. Each of them has its own advantages and disadvantages. In detail, it will be described in the next chapters. The second indication of the TAMD classification is the method of motor control. Two main approaches may be used here, such as the scalar control and the control based on the motor magnetic field vector. When the number of motors supplied by the single inverter is significant, the scalar approach is preferable. Nevertheless, it does not allow obtaining the dynamic motor characteristics of the same high quality as the vector approach gives. Examples listed above show the broad variety of decisions in the field of power circuits. They are dictated by such reasons as different supply voltages, different capacity of the used motors as well as the different types of power circuit switches.

#### **1.4 Conclusions**

Chapter 1 gives the state analysis and the development prospective of the TAMD.

1. Examples of drive power circuits are presented and analyzed, including a short description of TAMD applications. Based on this material, a classification of the drives in this field is proposed.
2. Significant differences in the traction multimotor connections are shown. Most of them are very bulky and do not have sufficient reliability though in the thesis detailed information was not collected due to the commercial confidentiality of the manufacturers.

## 2 STRUCTURAL-POWER SYNTHESIS OF TAMD

### 2.1 Structure analysis and configuration basis of TAMD

#### 2.1.1 Selection of configuration

This section is devoted to the structure analysis and the selection of the configuration for a drive based on the KT-4 tram example.

The KT-4 tram consists of two sections connected together by a so called “pleat”. Each of the two sections is based on the bi-axes bogie. Each tram axis is rotated via the gear by its own traction motor.

To avoid the high-cost works during upgrade of the mechanical part of the tram it is beneficial to save all available traction motors. Thus, three variants of the power unit configuration are possible. They are:

- a) each of the four traction motors is supplied by its own inverter,
- b) the motors of each bogie are supplied by the single inverter, that is a couple of motors obtain the supply from an inverter,
- c) four traction motors are supplied by the common inverter.

Comparison of the main indications of possible configurations is given in Table. 2.1.

*Table 2.1 Comparison of the main characteristics of possible traction drive configurations for the KT-4 tram*

	a)	b)	c)
Cost	maximum	mean	minimum
Control system complexity	minimum	mean	maximum
Dynamic and static characteristics	best	mean	worst
Reliability of the traction drive at all	maximum	mean	minimum

The data given in Table 2.1 show, that the best characteristics will allow the system with individual inverters of each traction motor with the exception of cost (variant a). It is clear because the control system may take into account

the individual parameters of each “traction motor-gear-wheel pair” system during the reference generation.

The main complexity of building the asynchronous traction drive lies in the rotational speed difference of the traction motors, which impedes the design of the control system for traction drive. The main reasons are follows:

1. differences in the traction motor parameters,
2. differences in the wheel diameters of separate tram axes.

By using the separate supply source, the individual voltage may be referred for each traction motor, allowing the motor operation with its own rotational frequency and slip. When the motor group is supplied by the common inverter, it is required to exclude the transition of the motors having the highest rotational frequency into the generator-braking mode. Due to the rotational speed difference, the load of the parallel-connected motors will also be uneven because of the different slip of separate motors. It may cause a significant underloading of some motors as well as the overloading of other ones. If the supply frequencies are similar, the motors having the highest speed will be less loaded because of less slip and vice versa.

To build the asynchronous traction drive with a group of induction motors supplied by the common inverter, the next conditions must be fulfilled [CTEП82].

1. limiting of traction motor parameter spread,
2. limiting of tram wheel diameter difference.

In the case of the asynchronous traction drive for the KT-4 tram, the common supply of all traction motors by the single inverter (variant c) is less expensive and most complex in implementation. Here, the required deviation of the wheel pair bands is to be sustained. During repair, this may lead to the selection of the wheel pairs among the full range of reserve sets that the tram enterprise has.

Based on this analysis and the comparison of principal solutions, the next solutions were found to realize the traction ac drive. As the traction motors, the squirrel-cage rotor induction motors were selected that have high technical parameters and relatively low cost. As the traction converter, an autonomous three-phase voltage inverter built on IGBTs was selected. In the terms of the control method for the traction drive, the vector control using the speed feedback sensor was selected. The optimum configuration of the KT-4 tram traction drive is “one inverter – two traction motors” for the bogie drives, that is two inverters must supply four motors. The drive block circuit is represented on Fig. 2.1.

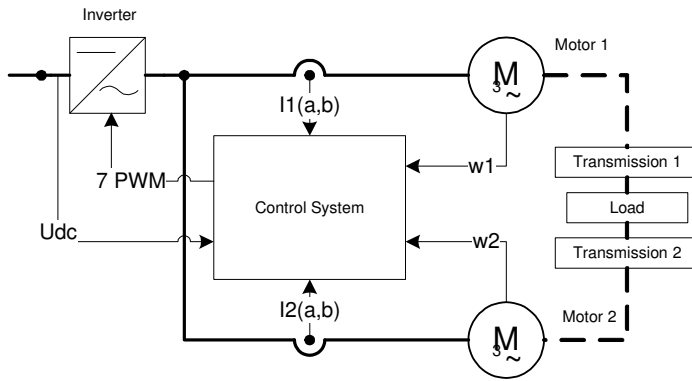


Fig. 2.1 Block circuit of the new drive

### 2.1.2 Drive model development

To process the control algorithms, the functioning model is to be designed including the real control system of the valuable drive. The model must be created in such a way that students could carry laboratory tasks in the future. All its components are selected with iterative stock to provide the model integrity in the case of supernumerary situations.

The model power circuit represents the three-phase voltage inverter (Larionov's bridge) built on the IGBT of Semikron Company. To control the transistor gates a specific driver is used which includes also the protection and diagnostic means. The smoothing choke is placed in the input, which forms the input LC filter together with the capacitor of the dc link. The model is supplied by the 600 V dc source. The braking transistor is set in the dc link in series with the braking resistor. The electrical circuit of the model power unit is shown in Fig. 2.2.

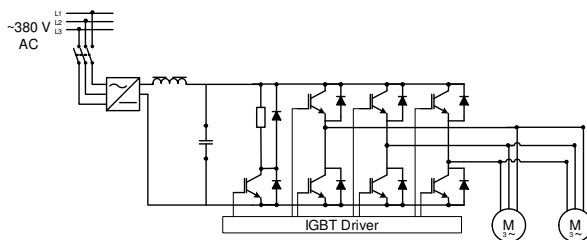


Fig. 2.2 Electrical circuit of the model power unit

The control system is built on the base of 32-bit TMS320F2812 processor of Texas Instruments. This DSP is distinguished by its high calculation speed, exceeding up to 150 MIPS. It includes an integrated analog-to-digital converter of 12-bit resolution. Two event managers control the three-phase bridge. The built-in logic modules allow direct connection of the pulse sensors without any auxiliary circuits. The CAN modules provide the DSP

control system integration into the on-board informational network of a tram [TEX02].

To obtain drive information, different parameter measurements are required. To measure the phase currents, the Hall-effect sensors are used. Four sensors are in use, the two of those serve each controlled motor. The third phase current is calculated using the first two currents. The dc link voltage is measured by the galvanically-isolated processor. This allows permanent control of the supply voltage as well as that of the braking chopper. Pulse speed sensors have 2048 pulse per round resolution.

### **2.1.3 Structure forming of KT-4 tram traction system**

For the power drive equipment of KT-4 tram, three kinds of power inverter and induction traction motor connections are commonly used.

An evident difference of these combinations is the number of inverters. This number may be one, two, and four, depending on the circuit. The difference concerns the used elements in the three different circuit variants. At the same time, the number of components does not define directly the cost of the device, which may be more or less expensive. Contemporary market of the semiconductor components and devices is broad-based, in terms of displayed components and price categories. For example, the overall cost of two inverters ACS550-01 of ABB at a motor load 37 kW is 5 % more expensive than the cost of 75 kW [ABB05].

With regard to the components of the switch elements, the cost of the 37 kW inverter production unit may exceed the cost of two 75 kW production units because it is more difficult to create more powerful components that have the highest frequency response.

Concerning tram traction converters, firstly underline the typical units of the drive link:

1. pantograph mechanism;
2. induction traction motors;
3. autonomous inverter consisting of:
  - protection apparatus,
  - input net filter,
  - regenerative braking unit,
  - communication module (execution unit),
  - servo system and the system for the communication unit control.

Before selecting the components according to points one, two, three, and five, the execution device must be selected, where it is possible to implement the vector control principle.

The components required by the variant built on the individual motor frequency converters are free accessible and interchangeable whereas other variants meet the problems in the element choice and search. When the passing currents are high, the components are of significant sizes, whereas the number of components grows fast at low currents.

Obviously, the variant built on the four autonomous inverters seems prospective at the moment and possibly, it will state the same time in the future. The only minus is the cost of the control system. Finally, the economy obtained from the use and the reduction of maintenance expenses both give significantly high prospects in contemporary economics. Additionally, the life cycle of the upgraded trams rises. From now on, the number of defects and outs of service depends on the external factors only, neither on the maintenance conditions nor on the modes of operation [RJA05]. Table 2.2 gives the comparative costs of drives having a different number of inverters.

Table 2.2 Comparative cost of different drive variants

Purchase part						Assembly part						Economic part							
Component	Manufacturer	Name	Number of inverters			Purchase cost of components		Pre-paring	Assem- bly	Connection			Revision	Overall cost	Overall cost	Overall cost			
			1	2	4	Price per unit	Overall cost			Con- tacts	Arma- ture	Cable					of 1 inverter	of 2 inverters	of 4 inverters
			Number of components																
Chokes	ELHAND	not in list	1			1400	1400	14	28	14	28	98	28	1610					
		ED1W-0,5/500		2		1000	2000	20	40	20	40	140	40		2300				
		ED1W-5,0/200			4	500	2000	20	40	20	40	140	40				2300		
Capacitors	EPCOS	B25655-A1148-K000				150													
	ICAR	LNK-P4X-2000-70	8			135	1080	10.8	21.6	10.8	21.6	75.6	21.6	1242					
		LNK-P4X-2000-70		2		135	270	2.7	5.4	2.7	5.4	18.9	5.4		310.5				
LNK-P8X-1500-70				4	95	380	3.8	7.6	3.8	7.6	26.6	7.6		437					
LNK-P3X-750-70				8	75	600	6	12	6	12	42	12				690			
Transistors	SEMIKRON	SKiiP 832GB120-4D	3			510	1530	15.3	30.6	15.3	30.6	107.1	30.6	1759.5					

		SKM 300GAL123D	2			300	600	6	12	6	12	42	12	690			
		SKiP 432GB120-2D		6		480	2880	28.8	57.6	28.8	57.6	201.6	57.6		3312		
		SKM 300GB123D		2		150	300	3	6	3	6	21	6		345		
		SKiP 232GDL120-4DU			4	480	1920	19.2	38.4	19.2	38.4	134.4	38.4			2208	
	SEMIKRON add-ons	Radiator	1			100	100	1	2				2	105			
				1		100	100	1	2				2		105		
Braking resistors	AS C33MO	BR1K2W6P8	48			110	5280	52.8	105.6	52.8	105.6	369.6	105.6	6072			
				48		110	5280	52.8	105.6	52.8	105.6	369.6	105.6		6072		
					48	110	5280	52.8	105.6	52.8	105.6	369.6	105.6			6072	
Braking interrupters	AS C33MO	VFD4045			250												
Disconnecter	ABB	S6N 800 FF 3.poles	1	-	-	620	620	6.2	12.4	6.2	12.4	43.4	12.4	713	713	713	
Contactator	ABB	AF 460-30-22	1	-	-	600	600	6	12	6	12	42	12	690	690	690	
Current sensor	ABB	ES1000	3			135	405	4.05	8.1	4.05	8.1	28.35	8.1	465.75			
		ES500		6		100	600	6	12	6	12	42	12		690		
		ES300			12	85	1020	10.2	20.4	10.2	20.4	71.4	20.4			1173	
													Summary	13347	14974	13846	

## **2.2 Comparative analysis and TAMD simulation tool selection**

### **2.2.1 Classification**

Computer simulation is the optimum method to obtain the description of the processes flowing in the existed or developed equipment.

The software used in the simulation may be divided into two parts. The first part discusses the simulation toolboxes whereas the second one deals with the soft tools for the control system programming and writing the “host“-programs for personal computers. The use of simulation software allows evaluating the future possibilities of the novel equipment before its creation.

Next, the programs used in the thesis will be briefly described.

### **2.2.2 Code Composer Studio 2.0**

The main soft tool for the signal processors is the Code Composer Studio 2.0 of Texas Instruments. The workshop of Code Composer Studio allows cutting the software coding time of the DSP systems. It includes the basic instruments for the DSP/BIOS real-time systems support and data visualization, the subsystem to analyze live data, the code generator as well as the interface to connect the modules of detached manufacturers.

The function libraries of the processor manufacturer are used effectively in the programming process. “Fast Mathematic Library” [IQM02] and “Drive Control Library” [DIG02] help to decrease the software development time. SDFlash utility from Spectrum Digital is used for the built-in flash memory execution.

### **2.2.3 Microsoft Visual C++ 6.0**

Microsoft Visual C++6.0 is used as the “host“-programs design tool. This software choice results from the Microsoft Visual C++ popularity among the designers of the majority worldwide toolboxes starting from Web explorers and ending by the time-dependent corporative applications. Visual C++ is the most effective and highly efficient C++ development instrument for Windows. Visual C++ brings the simulation to the new productivity level without flexibility, speed, and control lost [VIS04].

### **2.2.4 Matlab 6**

Matlab-Simulink is used for the simulation of the drive and control system operation. Simulink is an interactive tool of modeling, simulation, and analysis of dynamic systems. It opens the possibility to build the graphical block diagrams, to simulate the dynamic systems, to research system operation, and to improve the designs. Simulink is fully integrated with MATLAB, thus providing immediate access to the broad spectrum of analysis and design instruments. In addition, Simulink is merged with

Stateflow to simulate event-oriented behaviors. Thanks to these advantages, Simulink serves as the popular toolbox for the control and communication systems design, digital processing, and other motor simulation applications [MAT04].

### **2.2.5 PSCAD**

The toolbox PSCAD is suitable for the electrical process simulation of the converter-motor systems. It is a fast, accurate, and easy-to-use simulation tool for different electronic systems. The usage of the program allows checking the correctness of the selected converter elements, to study the influence of the power switches on the supply net, to find the rates of radio noise filter components.

### **2.2.6 Comparative analysis of the simulation tools**

Each of the discussed programs has its advantages and drawbacks. Next, they are discussed in detail.

PSPICE is best suited for the exact simulation of electronic circuits and their components. It contains the reach libraries of semiconductor components though the motor simulation is labored (the designer's own models are required). Moreover, often losing a step occurs during the simulation caused, obviously, by the mathematic apparatus of the differential equations solving, the tuning of which is a sufficiently laborious process. In general, obviously, the model simulation in PSpice causes more complications and problems in the differential equations solution than PSCAD does.

MATLAB is the well-known application soft tool, where different libraries for a broad problem spectrum solution may be used.

For instance, Simulink helps to describe the searched system by different kinds of transfer functions and feedbacks, thus giving a possibility to use the ready models and functions.

MATLAB/Simulink merged with PowerLib libraries has been designed especially for the electrical and electronic devices, schematics, and circuit development. Nevertheless, as the toolbox works in the MATLAB environment, it involves such drawbacks as the significant computer simulation time and often losing step during the solution of the non-linear differential equation systems.

### **2.2.7 Selection of the simulation tool**

As a result, the EMTDC/PSCAD (Power Systems CAD/Electromagnetic Transients DC) system was selected to simulate the power drive unit. This is a specially designed toolbox to simulate different electromagnetic processes in energetic systems, power electrical circuits, electronic and electromechanical converters.

It is based on the algorithm, which is stable to failing out of steps during the solution of differential equations in the simulation, thus allowing acquisition of the result sufficiently fast.

Matlab software was chosen for the drive control algorithms simulation. Today, many toolboxes exist to simulate the dynamic systems. Among a vast number of application tools, Matlab (The Math Works Inc.) takes the specific place. Primarily oriented on research projects, the system became the workhorse not only for researchers, but also for design engineers and students. In the communities of radio engineers, managers, physics, and telecommunication workers, Matlab obtained unusual spreading and practically became the mean of interdisciplinary and international communication. Matlab use is especially broad and effective in the field of signal processing, which involves computer science, communication, control, radio location and navigation, broadcasting and television, medicine instrument-making and measuring technique, auto and domestic electronics, etc [AHOX01].

## 2.3 Development and identification of the induction motor equivalent circuit

### 2.3.1 Equivalent circuit

One of the necessary conditions of the vector control system is the presence of the mathematical model of the right motor. The first step in the model design concerns the defining of the equivalent circuit parameters.

The main parameters of the induction motor are simulated by using the equivalent circuit. This equivalent circuit is suitable in the building of the induction motor vector control algorithms [LEON00]. Figure 2.3 displays a single-phase equivalent circuit, the parameters of which may be defined both theoretically and experimentally.

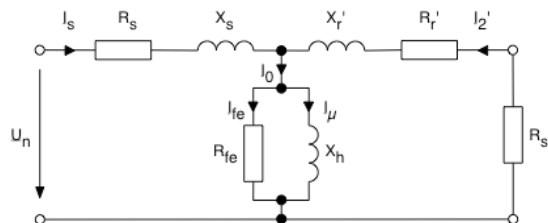


Fig. 2.3 Single-phase equivalent circuit of the induction motor

### 2.3.2 Experimental search of the equivalent circuit parameters

It is required to build the controlled three-phase voltage source to define the equivalent circuit parameters. Attempts to use the voltage obtained from the

frequency converter model were unsuccessful possibly due to the high-frequency noise in the converter. Three experiments were carried out, which included the measuring of Ohmic resistance of the motor, short-circuit experiments, and no-load experiments. In the short-circuit experiment, the induction controller was used that allowed the voltage control in the range of  $\pm 50$  V. Figure 2.4 displays the schematic image of the short-circuit experiment.

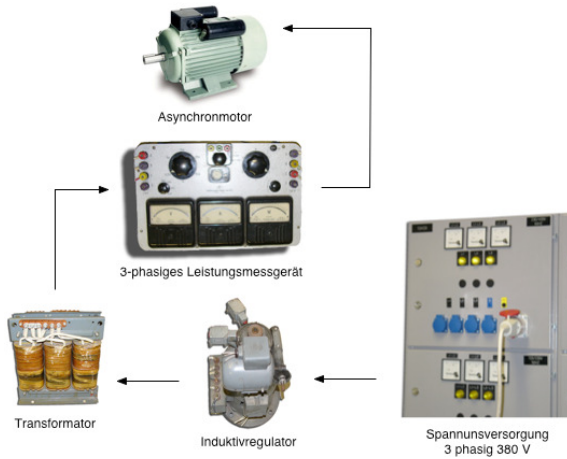


Fig. 2.4 Schematic image of the short-circuit experiment

### 2.3.3 Determination of stator winding resistance

Stator winding resistance was determined by measurements. Stator winding was supplied by the dc. In this case, the main inductance  $L_{\sigma} = 0$ . Using the Ohm's Law, the ratio of the voltage to current was defined, thus the winding Ohmic resistance was calculated.

### 2.3.4 Short circuit experiment

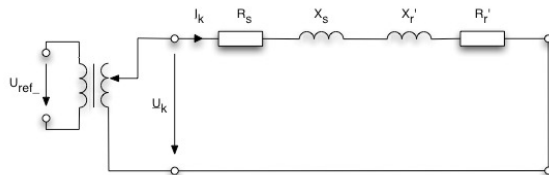


Fig. 2.5 Equivalent circuit of the short-circuit experiment

Short-circuited induction motor behaves similarly to the running motor. To provide for the measurement, the motor was blocked mechanically. Firstly, a measuring attempt was carried using the rated voltage. Nevertheless, this attempt led to a strong motor overheating, thus avoiding the pure measurement. Later, the motor was supplied via the transformer and

induction controller (Fig. 2.5). The voltage on the motor clamps was increased while the rated motor current was reached. The measuring results are given in Tables 2.3 and 2.4. Though the phase current values were different, they were considered symmetrical during the calculation. Therefore, the mean value of the three phases was used in the calculation.

When the slip  $s=1$ , that is in the short-circuit experiment, the resistances  $R_s$ ,  $X_s$ ,  $R_r$ , and  $X_r$  were less than the resistances  $R_{Fe}+R_{reib}$  and  $X_h$ . In that case, the motor's equivalent circuit may be viewed as the circuit shown in Fig. 2.5. From this, the resistances may be obtained.

### 2.3.5 Resistance calculation

The active resistance of the circuit was calculated using the single-phase active power and the short-circuit current:

$$R = \frac{P_{K(einph.)}}{I_K^2} \quad (2.1)$$

The reactive resistance of the circuit was calculated through the active and full circuit resistances:

$$X = \sqrt{Z^2 - R^2} \quad (2.2)$$

$$X = \sqrt{\left(\frac{U_K}{I_K}\right)^2 - R^2} \quad (2.3)$$

As the stator resistance is known, the rotor resistance  $R_r'$  may be calculated as:

$$R_r' = R - R_s \quad (2.4)$$

The calculation does not allow the separation of the stator and rotor resistances while the machine parameters are unknown. As an approximation, the rotor and stator resistances are accepted as equal:

$$X_s = X_r' = \frac{X}{2} \quad (2.5)$$

The rotor time constant is calculated as follows:

$$t_r = \frac{\frac{X_r + X_h}{2}}{R_r} \quad (2.6)$$

Table 2.3 Short-circuit experiment results under the rated voltage  $U_n=380$  V

Phase	$I_k$ [A]	$U_k$ [V]	$P_k$ [W]
A	7,5	228	1200
B	7	224	1100
C	7	226	1200
$\bar{x}$	7,167	226	1166,67

Table 2.4 Short-circuit experiment results under the rated current  $I_n=1,6$  A

Phase	$I_k$ [A]	$U_k$ [V]	$P_k$ [W]
A	1,62	62	66,3
B	1,58	61	65
C	1,59	61	65
$\bar{x}$	1,6	62	65,4

### 2.3.6 Open circuit experiment

To carry out a no-load experiment when the slip is equal to zero, the equivalent circuit is simplified, as Fig. 2.6 shows. Supply voltage is equal to the rated value  $U_n=380$  V. Then, the no-load current  $I_0$  and the no-load power  $P_0$  were measured (Table 2.5).

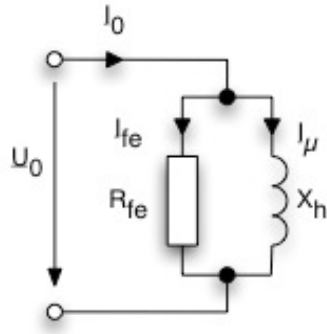


Fig. 2.6 Equivalent circuit of the open circuit experiment

Based on the obtained values, the circuit resistance may be found.

To calculate the resistance due to the steel and friction losses, use the following expressions:

$$R_{fe+Reib} = \frac{U_0^2}{P_0} \quad (2.7)$$

$$I_{fe+Reib} = \frac{U_0}{P_0} \quad (2.8)$$

To find the magnetization current, write the expression:

$$I_\mu = \sqrt{I_0^2 - I_{fe+Reib}^2} \quad (2.9)$$

Using the magnetization current, calculate the magnetization circuit resistance  $X_h$ :

$$X_h = \frac{U_0}{I_\mu} \quad (2.10)$$

Finally, calculate the mutual inductance  $L_h$ :

$$L_h = \frac{X_h}{2\pi f} \quad (2.11)$$

Table 2.5 Results of the no-load experiment:  $U_n=380\text{ V}$

Phase	$I_0$ [A]	$U_0$ [V]	$P_0$ [W]
A	1,55	228	50
B	1,38	228	60

C	1,45	228	65
$\bar{x}$	1,46	228	58,33

### 2.3.7 Theoretical calculations

The well known method of the calculation of the equivalent circuit of the induction motor uses motor's datasheet information. This calculation method is described by German-Galkin [ГЕР01].

The rated slip is calculated using the rated motor rounds-per-minute  $n_n$  and its synchronous rotational speed  $n_s$ :

$$s_n = \frac{n_n - n_s}{n_n} \quad (2.12)$$

The critical slip is calculated as follows:

$$s_k = (m_k + \sqrt{m_k^2 - 1})s_n \quad (2.13)$$

Running and rated torques ratio is as follows:

$$m_k = \frac{M_k}{M_n} \quad (2.14)$$

Mechanical losses are as follows:

$$\Delta P_m = \sqrt{3}I_n U_n \cos(\varphi)\eta - P_n \quad (2.15)$$

The rotor resistance is:

$$R_r' = \frac{1}{3} \frac{P_n + \Delta P_m}{(1 - s_n)i_k^2 I_n^2} \quad (2.16)$$

The full inductance is:

$$z_n = \frac{1}{2\pi f} \quad (2.17)$$

$$L_s = z_n \frac{\frac{U_n}{\sqrt{3}}}{I_n \sqrt{1 - (\cos(\varphi))^2 - \frac{\cos(\varphi)s_n}{s_k}}} \quad (2.18)$$

The rotor inductance  $L_{ls}$  is

$$L_{ls} = \frac{1}{4\pi f} \sqrt{\left(\frac{U_n}{i_k I_n}\right)^2 - (R_s + R_r')} \quad (2.19)$$

The mutual inductance is found as the difference:

$$L_h = L_s - L_{ls} \quad (2.20)$$

Table 2.6 Comparison of different methods of parameter definition

Parameter	Under the current limiting	Under the rated voltage	Theoretical calculations
$L_h$ [mH]	505	505	1140
$L_s, L_r$ [mH]	45,9	34,81	42,69
$R_{fe}$ [Ω]	891,21	891,21	-
$R_r'$ [Ω]	13,19	10,35	6,79
$t_r$ [ms]	41,77	52,15	174,18

An analysis of the obtained results shows that practical measurement gives a more exact picture than the theoretical approach suggests. Theoretical calculations may be used for the approximation search of the data of the motor equivalent circuit. In the case of the motor model design required for the vector control, practical data are preferable. In case it is technically impossible to define motor parameters directly by the inverter control system, the parameters may be preliminarily obtained in the laboratory conditions and saved in the system offline.

## 2.4 Simulation and research of the TAMD power unit

### 2.4.1 Simulation of the induction motor

Further to obtaining the equivalent circuit parameter values, the motor model may be created in Matlab. The Power Electronics library serves for this purpose. The library includes synchronous, induction, and dc motor models. Each machine model may be described both in absolute and per-unit frame. Universal Measurement Demultiplexer serves for the measuring of the needed motor state variables [SIMU13].

## 2.4.2 Simulation of the inverter

The Power Electronics library contains seven types of the separate power elements and the models of different semiconductor converters represented by the Universal Bridge.

In the tuning fields the following data may be entered:

1. the number of arms in the universal bridge (the field Numbers of bridge arms);
2. input and output ports configuration (the field Port configuration);
3. type of the power semiconductor component (the field Power Electronic device);
4. circuit parameters for building the switching trajectory are given in the fields of Snubber resistance and Snubber capacitance. The field of Measurement serves for the selection of the state variables of the universal semiconductor bridge.

Each semiconductor element includes an input (m) where the voltage and current shapes may be viewed and measured, using the measuring devices. All the units have the control inputs. For separate elements, these inputs are marked as (g) whereas for the universal bridge - as (pulses).

## 2.4.3 Simulation of the drive mechanical unit

Tram's mass is referred to the shaft of the single motor. For this, the equation of kinetic energy is used:

$$m \cdot (1 + \gamma) \cdot \frac{v^2}{2} = N_m \cdot J_{ekv} \cdot \frac{\omega^2}{2}, \quad (2.21)$$

where  $\omega$  - motor's rotating speed [rad/s],

$v$  - tram's linear velocity [m/s],

$N_m$  - number of traction motors,

$m$  - tram mass [kg],

$(1 + \gamma)$  - inertia factor of the rotating parts,

$J_{ekv}$  - equivalent moment of inertia.

The factor  $(1 + \gamma) = 1,09 \dots 1,15$  concerns the mass of a small carriage that increases due to the rotational mass inertia. Assume  $(1 + \gamma) = 1,12$ .

An equivalent moment of inertia is as follows:

$$J_{ekv} = \frac{1}{4 \cdot N_m \cdot u^2} \cdot m \cdot (1 + \gamma) \cdot D_r^2, \quad (2.22)$$

The equivalent moment of inertia depends on the carriage's mass, which in turn depends on the number of passengers. This number may be defined by means of statistics only. To simplify it, assume an average passenger mass 3,5 t (50 persons). Then, the carriage's gross mass is:

$$m_{brutto} = m + 3,5 = 19,8 + 3,5 = 23,3 \text{ t.}$$

The ratio of the linear velocity of the tram motion to the angle speed of motor rotation is expressed by the equation:

$$\frac{\omega}{\nu} = \frac{2 \cdot u}{D_r}, \quad (2.23)$$

where  $D_r$  - wheel diameter,

$u$  - gear ratio between the wheel and motor:

$$u = \frac{\pi \cdot D_r \cdot n}{60 \cdot \nu} = 7,43 \quad (2.24)$$

Then, using the equivalent moment equation, the equivalent moment of inertia may be calculated as follows:

$$J_{ekv} = \frac{1}{4 \cdot 4 \cdot 7,43^2} \cdot 23,3 \cdot 10^3 \cdot 1,12 \cdot 0,7^2 = 14,5 \quad (2.25)$$

The gear ratio between the motor angular speed and the tram's linear velocity is:

$$w = \frac{\omega}{V} = \frac{2 \cdot u}{3,6 \cdot D_r} \quad (2.26)$$

where  $V$  - motor linear velocity [km/h].

From the main dynamic equation, it follows that

$$J \cdot \frac{d\omega}{dt} = T - T_s, \quad (2.27)$$

where  $T_s$  - static torque

The static torque measured during the motion is raised depending on the speed. Taking into account the air resistance,

$$T_s(V) = 60 + 0,03 \cdot V^2 \quad (2.28)$$

## 2.5 Development of the calculation method of the traction motor power

### 2.5.1 Calculation method

Electric traction drives may be divided into groups using the next indications:

1. kind of traction motor (dc or ac);
2. structure of the power circuit (number of motors and converters, braking methods, and specific possibilities);
3. control circuits;
4. control methods;
5. methods of braking energy use and dissipation.

Different types of traction motors are displayed in Fig. 2.7 [JOL01].

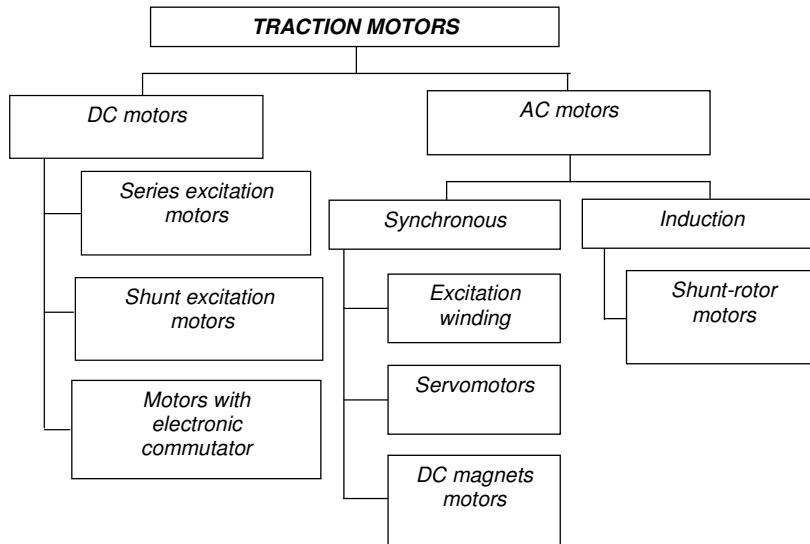


Fig. 2.7 Types of traction motors

To find the minimum required power of a traction motor (TM), the travel mode is examined, in which the electric train ЭП-2 of 220400 kg and the tram KT-4 of 25800 kg are running on the right railway path with the maximum possible constructional speed. Such a travel mode is chosen because in this case the maximum aerodynamic resistance force occurs, which is directly proportional to the square of speed, and the longitudinal

power is developed (unlimited motor operation power), which serves as the basic power for the motor in the proper operation mode.

The main parameters of an electric train and a tram required for the traction-energetic calculation are given in Table 2.7 [ТИХ02] [СТРО06] [КРАС06] [НА399].

Table 2.7 Initial data for calculation

Parameter	Value	
	ЭР-2	КТ-4
<b>Mass and geometric parameters</b>		
Full mass, kg	<b>220400</b>	<b>25800</b>
Width, m	3.522	2.18
Height, m	4.253	3.11
Midlevel section calculation factor	0.8	1.1
Midlevel section area, m <sup>2</sup>	11.98	7.46
<b>Constructional characteristics</b>		
Traction motor efficiency, $\eta_{ТЭД}$	0.95	0.95
Gear efficiency, $\eta_p$	0.9	0.9
Inverter efficiency, $\eta_{И}$	0.8	0.8
Maximum speed, km/h (m/s)	130 (36)	80 (22.2)
<b>Road-maintenance travel conditions</b>		
Maximum road slope, %	3	3
Gravity acceleration, m/s <sup>2</sup>	9.8	9.8
Specific air density, kg/m <sup>3</sup>	1.25	1.25
<b>Calculation factors</b>		
Friction factor of the rolling bearings	0.015	0.015
Friction factor between wheel ledge and rails	1.2	1.2
Wheel diameter, mm	1050	640
Wheel shaft pivot diameter, mm	0.2	0.2
Rolling friction factor	0.0007	0.0006
Wheel-rail coupling factor	0.2	0.2
Aerodynamic friction factor	0.6	0.6

Comment: The calculation factor of the tram midlevel section is increased due to the converter placed on the tram roof. Electric train's mass is defined from the configuration. In Estonia, it is two head and two motor carriages.

The head carriage's mass is 42.3 t. and that of the motor carriage is 57.9 t. The passenger and their burden weight should also be taken into account. For ЭП-2, assume 200 persons per 100 kg (with burden). The result is 20 t. For КТ-4, assume 60 persons per 100 kg, the result is 6 t. Slopes of the majority of railways do not exceed 1 % (i.e., the level overfall of the road-bed is 1 m on the length 100 m) per the horizontal length. The slopes that exceed 2% on the main railways are very rare though they may reach 3 % in the mountains. In practice, this means a slope no more than 1.7 degrees per 100 meters [КРҮГ05]. An electric stock is usually designed not for the definite line but for the common application in the railway net. The same concerns problems with a tram.

The uniform motion is obtained under the force balance:

$$\sum_{i=1}^n F_x = 0 \quad (2.29)$$

Thus, the overall motion resistance required to be overcome by a tram or an electric train is equal to

$$F_{\kappa} = F_f + F_w + F_{mp}, \quad (2.30)$$

where  $F_{\kappa}$ -wheel traction force,

$F_f$ -slope resistance,

$F_w$ -aerodynamic motion resistance force,

$F_{mp}$ -wheel rolling resistance force, H.

### 2.5.2 Calculation examples

Calculation examples are given in the full version of the thesis. The main data of the selected motors are given in Table 2.8.

Table 2.8 Obtained data of the motors for the ЭП-2 train and the КТ-4 tram

Parameter	ЭП-2	КТ-4
Maximum prolonged power, kW	194	40
Rated rotational frequency, rpm	961	1848
Maximum rotational frequency, rpm	2077	4925
Rated supply frequency, Hz	32,8	63
efficiency, %	≥ 90	≥ 90
$\lambda_m$	2,6...2,9	2,6...2,9
Cooling	independent	independent

Standard	IEC60349 – 2	IEC60349 – 2
----------	--------------	--------------

The data obtained are approximate character though their accuracy is sufficiently high for the technical and economic calculations.

### 2.5.3 Motor selection for Estonia

Following the results of the traction calculation, a motor may be selected from the model rows of different rolling stock manufacturers.

#### Special solution of ČKD PRAGOIMEX

Figure 2.8 shows the induction motor of the KT4 tram built by the Czech company ČKD PRAGOIMEX. This motor has proper parameters (Table 2.9) to be applied for tram and does not require any alteration [ČKD06].



Fig. 2.8 Induction traction motor TAM 1003 O

Table 2.9 Parameters of induction motor TAM 1003 O

Manufacturer	ČKD PRAGOIMEX
Motor type	TAM 1003 O
Rated power, kW	84.5
Rated voltage, V	425
Rated current, A	142
Rated frequency, Hz	70
Rated rotational speed, rpm	2062
Efficiency, %	91.2
cos $\varphi$	0.89

Other motor variants are included in the full version of the thesis.

#### Solutions for electrical train $\mathfrak{P}$ -2

To upgrade the electrical train  $\mathfrak{P}$ -2, among the existing variants, the following solutions may prove most appropriate. The Siemens project uses four LGA 1446 motor having the data included in Table 2.10. Its appearance is shown in Fig 2.9 [SIM].



Fig. 2.9 Induction traction motor ALSTOM 4 LGA 1446

Table 2.10 Parameters of the induction motor 4 LGA 1446

Manufacturer	Siemens
Motor type	4 LGA 1446
Rated power, kW	180
Rated voltage, V	750
Maximum torque, Nm	1120
Standard	EMO 380
Maximum rotational speed, rpm	5080

Other motor variants are given in the full version of the thesis.

As the above given review shows, it is difficult enough to find the motor among the existing solutions that would fully meet the required characteristics. Even it meets the complete requirements, a significant alteration of the mechanical part is needed, particularly, the binding slots, gearbox, etc. Possibly, the re-arrangement will be required, which leads to additional expenses.

In this situation, specially manufactured squirrel-cage rotor induction motors are preferable, which fully meet the calculated technical data. The main advantages of this solution are as follows:

1. they avoid high-cost alterations in the mechanical units;
2. reduced price of the separate traction motor in the case of the high number of upgraded trams and the corresponding number of motors.

Such a solution for the KT4 tram was realized by VEM Sachsenwerk GmbH. The motors DKABZ 0305 – 4 are manufactured by the alteration of regular traction dc motors into the ac squirrel-cage rotor induction motors. Main data of the developed and the regular TE 022H motor are compared in Table 2.11.

*Table 2.11 Comparison of the main characteristics of the traction motors TE 022H and DKABZ 0305 – 4*

	TE 022H	DKABZ 0305–4
Rated power, kW	40	42
Efficiency, %	88,9	89,6
Rated speed, rpm	1460	1750
Maximum speed, rpm	4200	3941

The single motor DKABZ 0305–4 costs approximately 10000 EU. During the alternation, each tram requires four motors of such kind, i. e. the expense of the traction motors is close to 40000 EU. These expenses may be considered as unwarranted in some cases.

As an alternative solution, the design and manufacturing of the induction traction motors in an Estonian enterprise may be suggested. It will allow producing a motor having the most appropriate characteristics for the solution of the modernization problem concerning a tram. Among the Estonian electrical engineering companies that are in the electrical machine business, the Volta Company may be mentioned. This company has extensive experience in the field of electrical machine manufacturing.

## **2.6 Traction calculation of the tram motor drive**

### **2.6.1 Problem definition**

In the selection of the traction motor model, first, the main parameter concerning the renovated tram must be defined. These parameters will help to select a motor from the model row of a rolling-stock manufacturer and to prepare the project specification for the traction motor manufacturing by an Estonian enterprise.

To define the required power, the traction calculation is to be performed. The traction calculation gives the required power in the next modes:

1. rated mode (S1),
2. acceleration mode,
3. braking mode.

The rated mode is one of the motion mode sets needed for the motor calculation. The indications of this mode must be defined based on the motion cycle analysis. The rated mode is being processed during the traction motor design.

The acceleration and deceleration are the extreme conditions of the traction motors. The requirements to the braking system can be determined during the selection of motors and converters. In the traction mode, the converters

do not use full power because the high acceleration acts negatively on the passengers. At low velocity, large traction under low currents may be provided. Among the possible braking modes, the regenerative and the dynamic braking are considered. As far as the motor heating is concerned, both modes are equivalent, because in both cases under the referenced deceleration the braking energy does not dissipate in the motors but it returns to the supply net, excluding motor losses in the regenerative braking or dissipation in the braking rheostats.

## 2.6.2 Development of the motor mode calculation method

To clarify the motion character of a tram, the traction balance is to be prepared, which gives the summary motion counter-force. The traction balance equation for a tram is

$$F_{comp} = F_{mp} \pm F_{nod} + F_g \pm F_{dun} \quad (2.31)$$

where

$F_{comp}$  – tram motion total counter-force, N,

$F_{mp}$  – wheel rolling counter-force, N,

$F_{nod}$  – slope counter-force, N

$F_g$  – tram motion air counter-force, N,

$F_{dun}$  – tram inertia force, N.

All calculations are given in the full version of the thesis. Motor parameters were obtained by the calculations. The main data for the motor are presented in Table 2.12.

*Table 2.12 Main required data of induction traction motors for KT- 4 tram and KT – 6 modification*

	KT – 4	KT – 6
Rated power, kW	48,6	67
Rated rotational frequency, rpm	1848	1848
Maximum rotational frequency, rpm	4088	4088
Rated supply voltage frequency, Hz	63	63
Rated voltage, V	424	424
Voltage rate speed, kV/μs	0,8	0,8

Efficiency, %	≥90	≥90
Maximum power in the braking mode, kW	67	91
Maximum power in the running mode, kW	71	82
$\lambda_m$	2,6...2,9	2,6...2,9
Cooling	independent	independent
Cooling air consumption, m <sup>3</sup> /min	7,5	7,5
Standard	IEC60349 – 2	IEC60349 – 2

Isolation is selected according to the standard IEC60349 – 2 [IEC60349].

According to the data given in Table 2.12 the KT – 6 tram needs in more powerful motor than KT – 4 does. It may be impossible to acquire the required power of KT – 6 in the given frame. A solution may be to obtain the maximum possible power by using the isolation that has a high work temperature, for instance of 200 and 220 class, with some decrease in the tram dynamics.

The obtained data are approximate though their accuracy is high enough for the technical and economic calculations.

### **2.6.3 Development of the calculation method for the traction motor generator modes**

All the above-mentioned statements concern the motor mode of the machine, in which the motor torque and speed have an equal sign.

Both a directly supplied and the inverter-supplied ac motor one may operate in a generator mode. Nevertheless, the standard inverter cannot return energy to the supply line, because its uncontrolled input rectifier passes the current in one direction only. The return current flows exclusively in the case of the expensive B4 current rectifier usage. It does not seem beneficial in the case of low power applications. During the braking energy generation into the supply line, local overvoltages may occur that have negative effect on the supply line, thus deteriorating its parameters.

When the braking modes are analyzed, the main calculated variables are: Ohmic resistance of the braking unit, maximum braking power, and the rated braking power.

For the purpose of the braking equipment selection, calculation of the parameters of the mode is given in the full version of the thesis.

The summary of this calculation is as follows. In the dynamic braking, electric energy dissipated by the braking module is equal to 51.7 kW with the rated motor power 75 kW. In that case, the braking unit resistance does not exceed 6.98  $\Omega$  and the rated power of the braking resistor link has to be 7.4 kW.

#### **2.6.4 Development of the method for the braking unit calculation**

To realize the dynamic braking, the components of AS “Северо-Западное Электромеханическое Объединение” (ЗАО СЗЭМО) [ТЕХП05] have been selected. An external braking module and braking resistors are required to provide forced motor braking of the converters, the capacity of which exceed 15 kW. Recommended braking units and resistors are useful for the 10% braking cycle (the maximum braking duration is 10 s). The braking resistors BR1K2W6P8 have the rated data:

1. full resistance 5.8  $\Omega$ ,
2. overcurrent 125%

To control four induction motors using a single frequency converter,  $4 \times 16 = 48$  braking resistors have to be installed in series and the IGBTs of SEMIKRON SEMITRANS™ should be replaced by eight braking interrupters VFD4045, if possible; this way is certainly unsuitable.

In the variant based on the two frequency converters in the tram motion drive, a similar situation as in the previous case takes place but the braking converters may be avoided if an individual control system is introduced to commutate the transistor switches SEMIKRON SEMITRANS™.

The most favorable variant requires separate converters to supply each induction motor. In this case, each SkiiP transistor module integrates its own braking unit and the only add-on concerns the installation of 16 braking resistors for each motor.

### **2.7 Conclusions**

In the chapter, a new method of the structural-energetic TAMD synthesis method has been developed and tested on the example of KT4 tram.

1. In the first part of the chapter, the analysis of possible TAMD configurations was made and their systematization was proposed.
2. Using the analysis conducted and the comparison of possible principal solutions for the implementation of the tram traction drive, the novel engineering solutions were suggested. As the traction motors, the squirrel-cage rotor induction motors were selected because of their high technical features and relatively low cost. As a traction converter, the autonomous three-phase voltage inverter built on IGBTs was selected. As the method of

the traction drive control, the vector control with the feedback speed sensor is used. The optimum configuration of the KT-4 tram traction drive is the “one inverter – two traction motors” system for the drive of each bogie i.e. two inverters per four motors.

3. In the second part of the chapter, a comparative analysis was made and the TAMD simulation instruments were selected. The analysis showed that different soft tools are required for the simulation of various aspects of the drive execution. Particularly, to simulate the control system operation and to tune its algorithms, the MATLAB was suggested. To simulate electric processes, the PSCAD toolbox was recommended.

4. Next, equivalent circuit development and identification for induction motor is discussed. A comparative analysis was performed concerning various ways of obtaining equivalent circuit parameters. Both practical and theoretical approaches are examined.

5. The design and testing of the method for the TAMD induction motor was supported by calculation and component selection. In the calculations, the data of KT-4 tram and ЭР2 electric train were used. Using the results and the analysis of the motors in the market, replacement the existing dc motors by the ac ones was estimated.

6. The method of the drive traction calculation has been suggested, including the generator mode and the inverter braking unit calculations.

## **3 DEVELOPMENT OF THE DESIGN METHOD FOR THE TAMD FREQUENCY CONVERTERS**

### **3.1 Analysis of the methods and tools for the TAMD frequency converter control**

#### **3.1.1 Problem statement**

The control system of the traction drive serves as an instrument that provides the required functioning of the “converter – motor” set which performs the needed drive operation modes having the referenced dynamic and static properties.

As stated above, an autonomous inverter serves as the source of the supply voltage for the traction induction motor. To control the speed and torque in the “autonomous inverter – squirrel-cage rotor induction motor” system, the next main methods are commonly used:

1. scalar frequency control,
2. vector control called also a frequency control built on the field orientation principle,
3. direct torque control.

In addition to the drive speed and torque control that provides the required characteristics, the control system of a traction drive has to provide the following functions:

1. protection from the abnormal modes of the inverter and traction motor operation,
2. diagnostics of the main units of the traction drive,
3. signaling concerning the required values,
4. adjustment of the tram traction force depending on the rail-wheel coupling as well as the protection of the traction drive from skid and slip modes.

The contemporary control systems of electric drive are built on the microprocessor basis. The most suitable microprocessor type for the motor drive control systems is the compound signal processor, DSP. Major advancement in the DSP technology has taken place in the last decade. The modern DSP allows an implementation of the complex algorithms of the drive control at maximum speed. Analysis and selection of the appropriate processors is beyond the scope of the thesis because this problem concerns

equipment selection. Nevertheless, it may be shown that one of the modest models of Texas Instruments – TMX320F2812 - is recommended for the control system of the KT– 4 tram asynchronous traction drive. This processor may execute the frequency control of two asynchronous drives simultaneously.

### 3.1.2 Selection of the control principle for the traction drive

Comparison of typical features and main static and dynamic properties is given in Table 3.1. The table is arranged using the data given in [NASH97].

*Table 3.1 Comparison of the main characteristics of different control methods for the “autonomous inverter – squirrel-cage rotor induction motor” system*

	Scalar frequency control	Vector control	Direct torque control
Torque control	Indirect	Direct	Direct
Motor magnetic flux control	Indirect	Direct	Direct
Motor torque control error, %	±12	±4	±4
Time response of the torque control input, ms	150	10...20	1...2
Speed control error in the steady-state mode, %	±1...3	±0,01	±0,01

Following the given review of the frequency control algorithms for the squirrel-cage rotor induction motor and data in Table 3.1, the following conclusion may be drawn. The controllability of the scalar frequency control of the asynchronous drive is significantly lower than the vector and direct torque controls. The main arguments that prove this statement are as follows:

1. indirect motor torque and magnetic flux control,
2. significantly longer response time on the reference input signal than with the vector and direct torque controls.

In the traction drive, the reference signal of the tram control system is the traction force that is the drive torque. As shown above, in the scalar frequency control the torque is referred indirectly, on the basis of  $U=F(f)$  dependence, thus at the same time with the referred torque the motor magnetic flux changes. Such an obstacle is extremely limited for dynamic drive possibilities on the low traction motor shaft rotational speeds, which may causes the wheel pair slip in the running and the skid in the braking mode. When the motor vector control or the direct torque control is used, the torque and magnetic flux may be adjusted independently, thus allowing more accurate input reference performance.

As a result, the vector and direct torque controls are most appropriate for the tram asynchronous traction drive. Direct torque control is the fastest method of the asynchronous drive control because, its algorithm is simpler than with the vector control. Nevertheless, method of implementation of the the direct torque control presents a number of engineering difficulties.

That is why an optimum solution for the tram traction drive is the vector control method. It yields to the direct torque control method for speed and algorithm complexity though its implementation, as proved by the worldwide rolling-stock manufacturers' experience is simplest. The majority of the rolling stock is manufactured with an asynchronous drive with the vector control.

### **3.1.3 Problem statement of vector control in parallel coupled traction induction motors**

Based on the analysis of the three possible configurations of the asynchronous traction drive, the circuit "one inverter - two traction motors of the separate bogie" was selected as an optimum system. To control the "inverter - squirrel-cage rotor induction motor" system, the vector control with the rotor speed sensor was selected. At the same time, significant difference occur in the an implementation of the vector control algorithm for two parallel-connected motors and the usual vector control system of the single motor.

These systems were examined with an assumption of the equivalence of both motors, which will not cause any errors into the results because the parameter dispersion of the traction motor is strictly limited, as shown above. Using this assumption, of the vector control of the two parallel-connected squirrel-cage rotor induction motors can be realized with any algorithm that supports the equal electromagnetic torque of the motors, even if their rotational speeds differ.

To execute the vector control of induction motors that have high dynamic characteristics, exact information concerning the angle position of the spatial position of the flux vector is required because this angle is used for the axes

orientation. In the system “one inverter – two traction induction motors”, two variants of the required value calculation exist if the mathematical model is based on the determined full order observer:

1. average model of both motors,
2. calculation of the angle positions of the required flux vectors for each of the two motors is based on their individual models to be used in separate motor control algorithms.

In the first case, the model input signals are calculated using the mean current and rotational speed values. The output signal shows the vector position of some abstract averaged flux required by the motor. The model equations for this variant are the same as in the case of the usual single motor vector control.

In the second case, each motor uses its own observer. This solution is more complex than the first one though it has some advantages:

1. according to [PENA02], this variant gives a more accurate result of the required variable calculation;
2. the first variant excludes the motor parameter identification. The use of averaged values does not allow a degree estimation of the working magnetic flux saturation and a variation in the rotor’s active resistance because traction motors develop different powers at approximately equal torques;
3. in the tuning process of the vector control system, model factors of each motor may be measured with high precision using special test benches;
4. vector control algorithms for two parallel-connected induction traction motors can be realized if information of the fluxes of the motor rotor is known, with an exception of the averaged motor control.

Thus, to define the position of the reference flux vector, separate traction motor models are recommended for use.

In [PENA02], four variants of the vector control systems are described for the two parallel-connected traction motors supplied by the common inverter:

1. an averaged drive control,
2. switched drive control using the “leading-driven” principle,
3. mean control of two motors,
4. mean and differential control of two motors.

Below the listed methods are described in brief.

### An averaged drive control

An averaged drive control principle illustrated in Fig. 3.1 assumes the use of the reference signals of both motors to represent an “abstract averaged motor” having “averaged motor variables”. This principle may be realized by using the two principles listed above concerning the required flux position search. However, as shown above, it is advisable to apply the individual models of each traction motor to calculate the required value of the flux vector position. The input values of the vector control algorithm are the following average values: required flux vector positions, current, and motor speed. Based on these data, the standard algorithm of the vector control derives the required vector instant voltage, which supplies both motors. A similar way of control was suggested in [MATS01] where the number of parallel-connected motors may reach two and more.

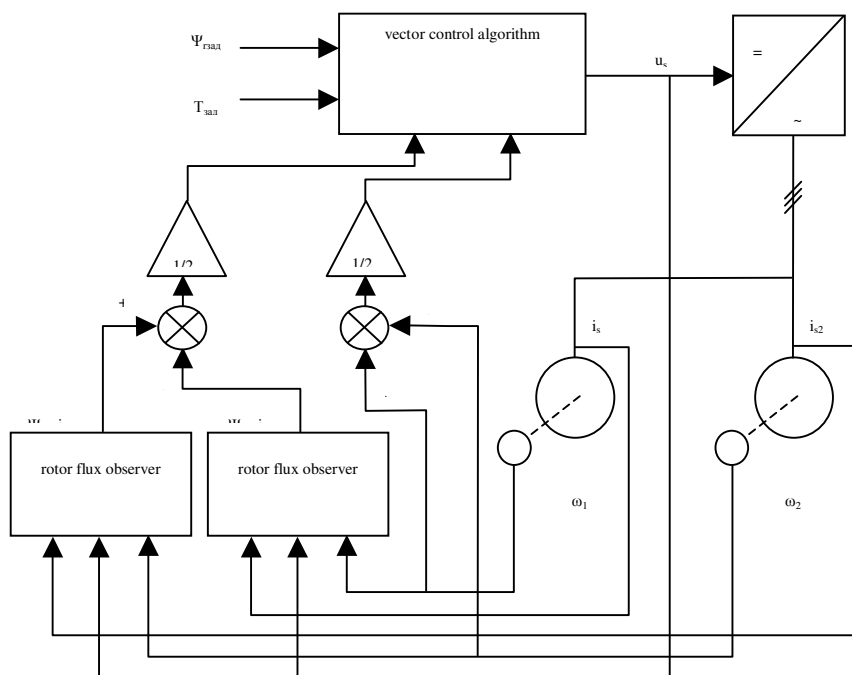


Fig. 3.1 Averaged drive control

### Switched drive control based on the “leading-driven” principle

Figure 3.2 illustrates switched drive control based on the “leading-driven” principle. In this principle, the measured and calculated signal of each motor alternately enters the input of the standard vector control algorithm. This is achieved by the use of multiplexers that allow one to find the position of each motor in the given calculation period. During a certain period, the control algorithm takes the signals of the single motor called “leading”

whereas another motor called “driven” is not considered. In the next derivation period, the motors switch the roles. Accordingly, the vector control algorithm calculates the voltages required by one of the two motors in each calculation period. In that situation, both models have to provide calculations uninterruptedly though during the derivation period the data concerning one drive only are used.

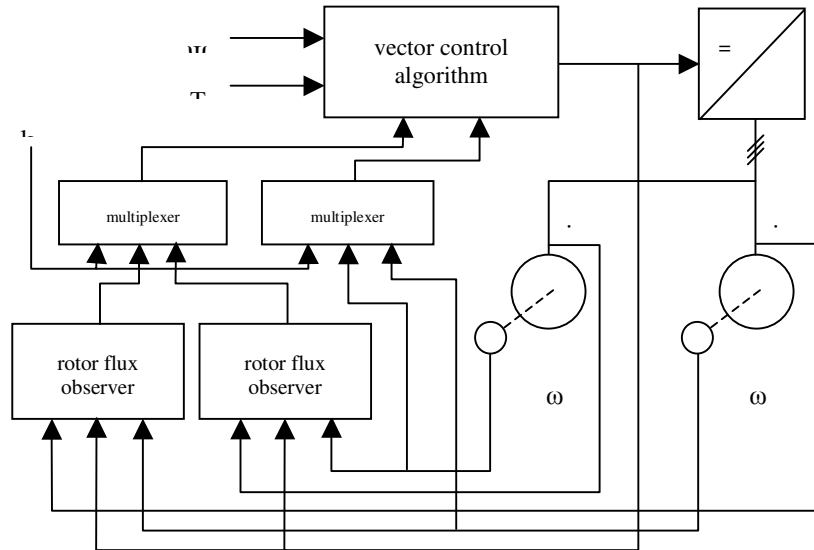


Fig. 3.2 Drive control based on the “leading-driven” principle

### Mean control of two motors

In this case, the control of each induction motor using the vector control algorithm is executed within the single calculation period, as Fig. 3.3 shows. The inverter control signals are produced here through averaging of the two signals calculated by the vector control algorithm of either of the two motors. This algorithm takes longer derivation than with other algorithms because a simultaneous calculation of two control processes is required.

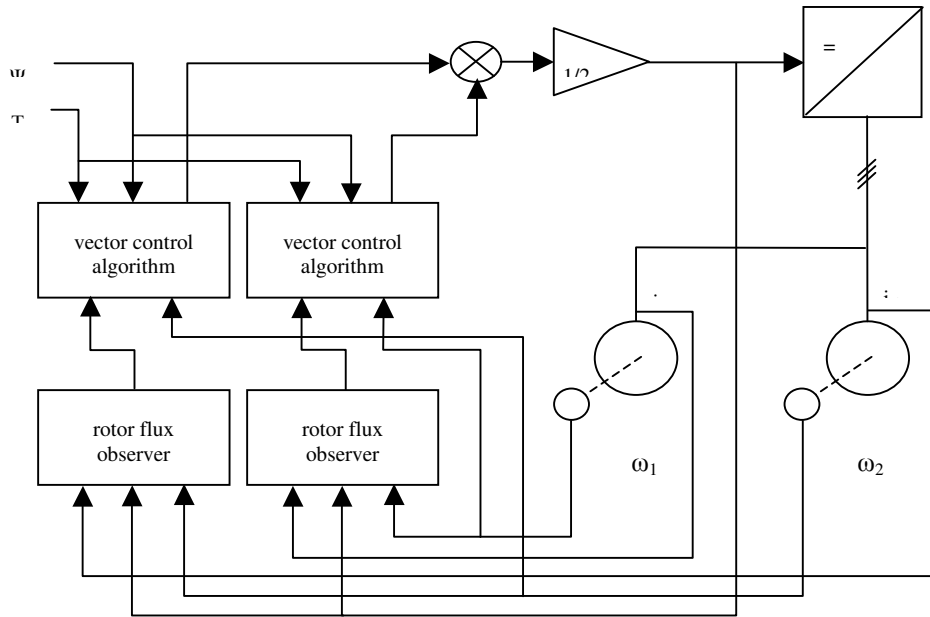


Fig. 3.3 Mean control of two motors

### Mean and differential control of two motors

The modified vector control algorithm is the basis of this control method (Fig. 3.4). The control method adjusts along the field-oriented axis not only the flux as in the usual vector control algorithm, but the motor torque difference also. The mean torque is adjusted along the field-perpendicular axis. To realize the algorithm, specific transfer functions connecting the axes-oriented variables are used.

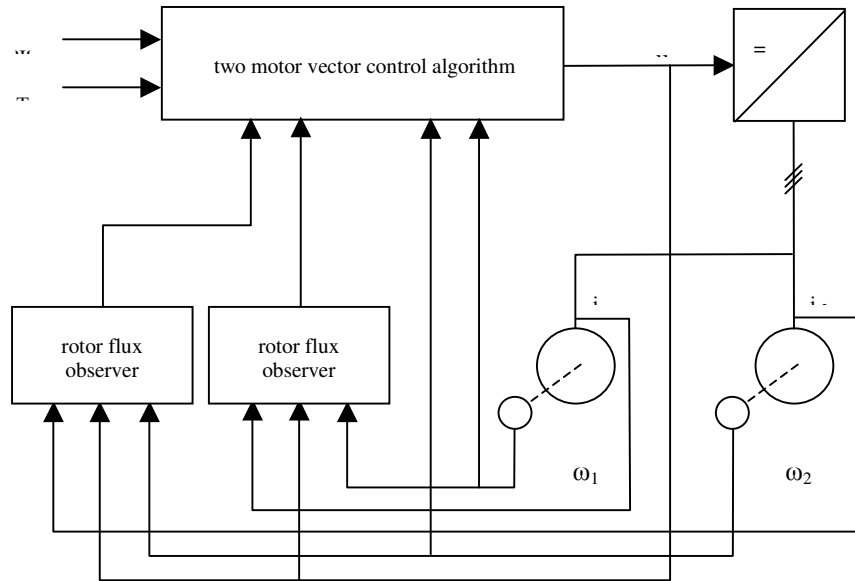


Fig. 3.4 Mean and differential control of two motors

In [PENA02], the dynamic properties of the four discussed methods are compared for the vector control of the two parallel-connected traction induction motors supplied by the common inverter. The comparison is based on the simulation results for each algorithm. In accordance with this research, the averaged drive control method shows the best dynamic properties. At the same time, it is the simplest and the quickest among the methods examined.

To sum up, it is still too early to draw final consideration. In the simulation, the following problems have not been discussed:

1. an interaction of the vector control system and the traction force adjustment system provide the maximum use of the coupling forces;
2. mechanical unit parameters (traction force transmission from the traction motor to the rail) considered as equal for both motors that is the possible difference in the wheel bandage diameters was not taken into account;
3. among the distortions that affect the traction drive systems the only ones examined were the wheel pair slippage and different axes loading, whereas other kinds of distortions were not considered.

Hence, in view of the above listed factors, additional research is required for the final selection of the vector control algorithm for the induction traction drive of KT-4 tram.

### 3.1.4 Model of Multimotor Drive with Frequency Converter

To implement conclusions resulted the previous chapter, we will consider the mathematical model of an induction traction drive having two motors.

Figure 3.5 shows the motor drive block circuit. A pair of parallel-connected motors is supplied by the common voltage inverter. To control the drive, the digital control system is used, which obtains data from different sensors of the drive. Three kinds of sensors are used: current sensors, voltage sensors, and rotational speed sensors.

All the motors have an identical transmission system which passes the torque to the wheels. The load is represented by the vehicle dynamic model.

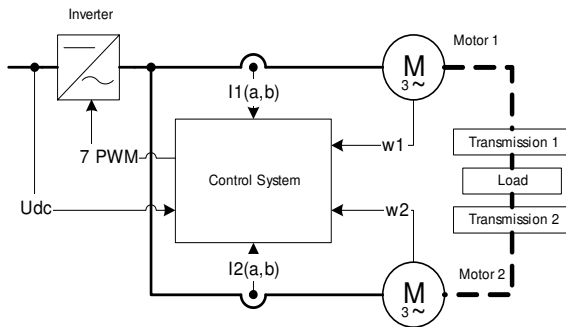


Fig. 3.5 Drive block circuit

To check and compare different control algorithms a typical situation was simulated for the four-motor KT-4 tram. In the starting instant, one of the axes loses coupling with a rail. From now on, the load of one of the motors consists of the friction force of motor bearings and transmission only. The moment of inertia is equal to the total rotor and transmission moments of inertia. The load of the second motor rises to 133 % (it is assumed that the load spreads between the rest of three motors). The shaft moment of inertia increases to 19,3 kgm<sup>2</sup>.

The traction drives require good inspection of the torque on the motor shaft. It is provided by the vector control, which needs to be adapted to the multimotor drive.

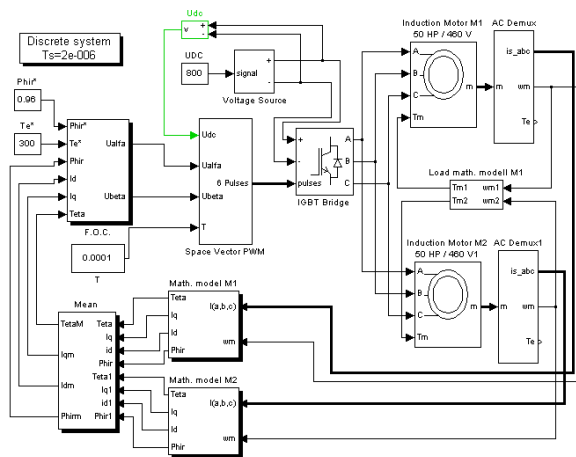


Fig. 3.6 Motor mathematical model in MATLAB

The motor mathematical model operates in all four quadrants. An electrical section of the machine is represented by the equations of the fourth order whereas a mechanical section – by the equations of the second order. All electrical parameters are referred to the stator. The model excludes an effect of steel saturation. [MATR13]

The following parameters have been used in the simulation:

1. power: 37.3 kW,
2. rated voltage: 460 V,
3. rated frequency: 60 Hz.

IGBT inverter model represents the classic three-phase bridge.

The space-vector PWM allows the required voltage vector to be obtained. Eight different base vectors exist, as shown in Fig. 3.7.

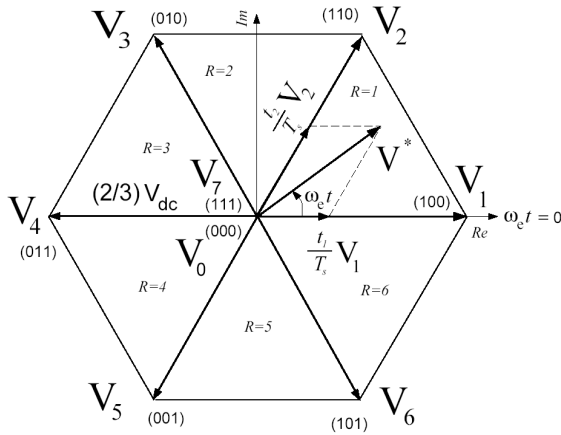


Fig. 3.7 Vector PWM

Vectors divide the circle by six sectors. Depending on the voltage required, switching combinations of the determined base vectors within the period  $T_s=t_1+t_2$  [FOC98] may be obtained.

In some cases, especially when the motor's rotational speed exceeds the rated value, there is no sufficient voltage on the vector buses. Therefore, Fig. 3.8 represents three popular methods of how to obtain the additional voltages [AHME97]. Particularly, the «minimum phase error» method is used in the space-vector PWM unit.

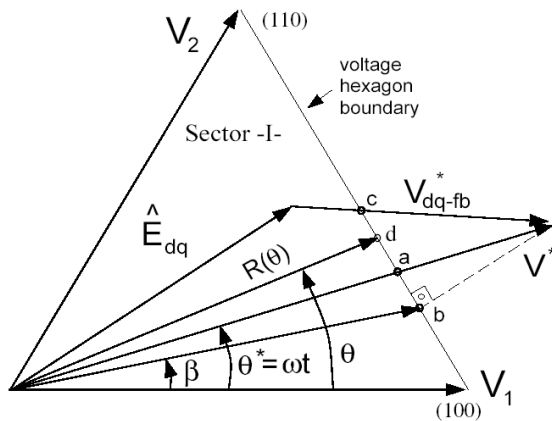


Fig. 3.8 Popular methods to obtain an additional voltage:  
*a: «minimum phase error» method, b: «minimum amplitude error» method, c: «dynamic field weakening» method*

The load model is shown in Fig. 3.9.

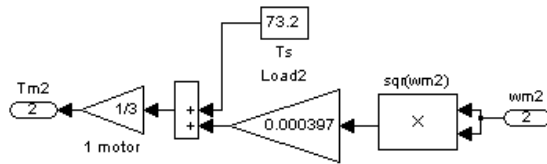


Fig. 3.9 Load model

When one of the axes fully loses contact with the rail, the load dissipates between the rest of the motors. All the parameters for calculations were obtained from [TIX02] and [KY302].

### 3.1.5 Analysis of the Frequency Converter Operation in the Multimotor Drive

The developed model was used for the simulation of the mean current control mode, the mode of two-model switching, and the averaged vector control algorithm.

The first method is based on the two equal motor models. Then, two motor models are averaged to obtain the mean motor model. The structure of the algorithm is displayed in Fig. 3.6.

To arrange models switching in the vector control mode, the data are obtained from the motor current model. This vector control algorithm collects data alternately from each current model. The structure of the algorithm is shown in Fig. 3.10.

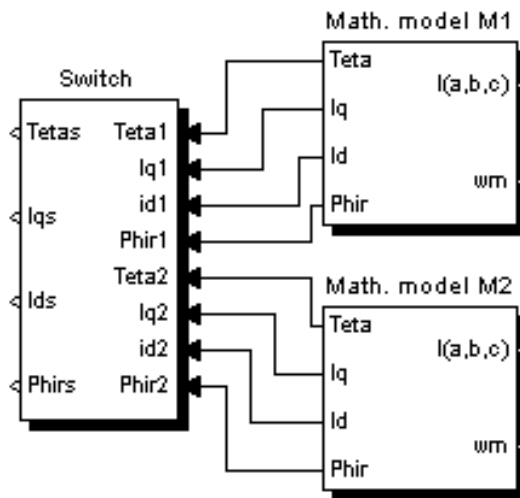


Fig. 3.10 Switching between models

The structure of the simplified vector control algorithm includes two motor current models and two vector control algorithms. Each vector control algorithm generates a control action, the averaged value of which supplies the inverter. The structure of the algorithm is shown in Fig. 3.11.

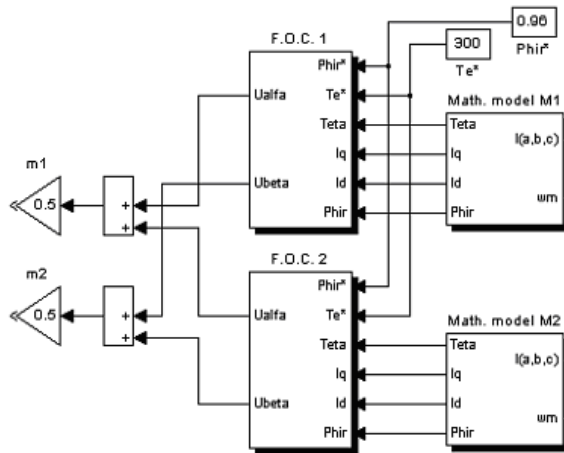
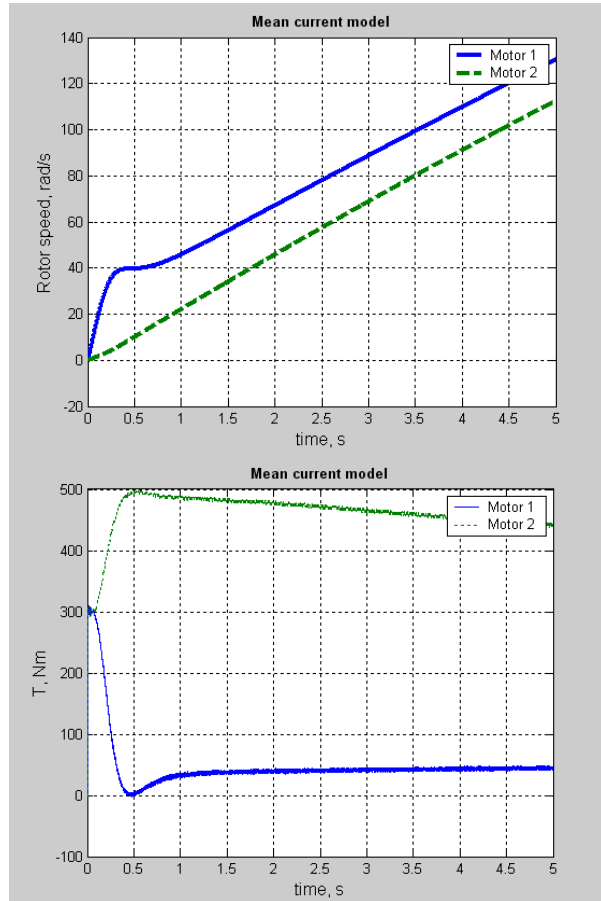


Fig. 3.11 Averaged vector control algorithm

For simulation Matlab-Simulink software was used. The following parameters were used in the simulation:

1. fixed-step Runge-Kutta fourth order method,
2. step: 2 ms,
3. simulation time: 5c,
4. PWM modulation: 10 kHz,
5. required torque: 300 Nm,
6. supply voltage: 800 VDC.

Simulation results of the mean current control are given in Fig. 3.12. The difference of rotational speeds in three seconds approaches ~20 rad/s. An error of the loading motor torque reaches 200 Nm of the referred value. Both motors have no sharp torque oscillations.



*Fig. 3.12 Simulation results of the mean current control*

Simulation results of the switching models are given in Fig. 3.13. Differences in the rotational speeds in three seconds approach  $\sim 15$  rad/s. An error of the loading motor torque reaches 350 Nm of the referred value. Both motors have sharp torque oscillations.

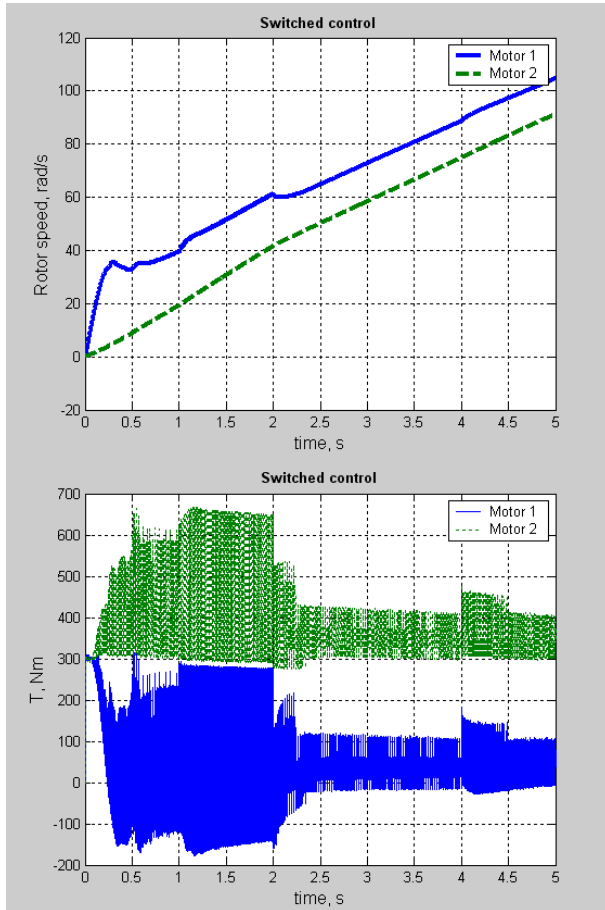


*Fig. 3.13 Simulation results of the swithing models*

Simulation results of the averaged vector control algorithm are given in Fig. 3.20. Differences in the rotational speeds in three seconds approach  $\sim 15$  rad/s. An error of the loading motor torque reaches 50 Nm of the referred value. Both motors have no sharp torque oscillations.

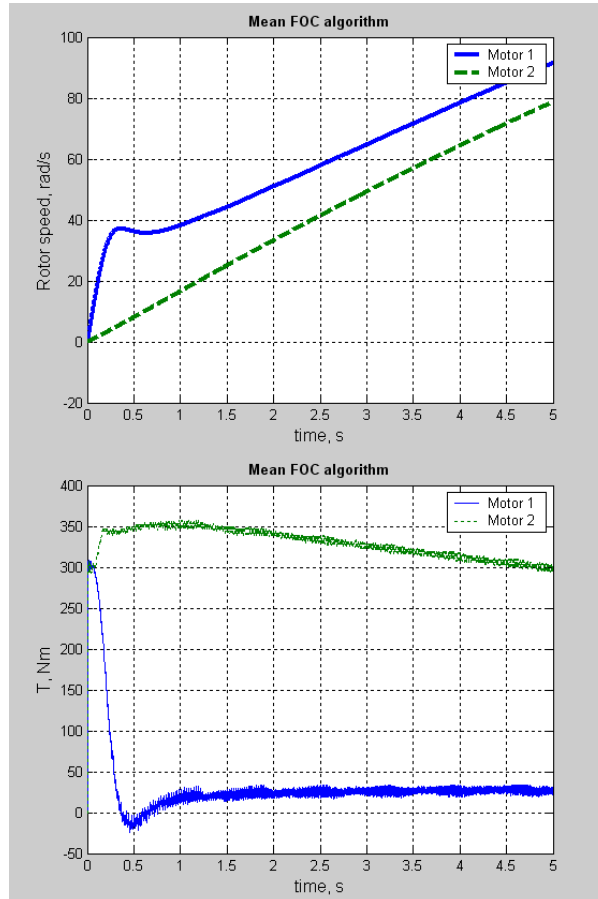


Fig. 3.14 Averaged vector control algorithm

As the simulation results of different control methods show, the most suitable control method is the «Averaged vector control algorithm». This algorithm allows development of the required torque with minimum error if the motor is in good contact with a rail. Nevertheless, this method does not solve all the problems. Further research as well as more complex algorithm and perfect model development are required.

### 3.2 Development of the circuit design method and power switch selection for the TAMD converter

#### 3.2.1 Selection of controlled switch types

For the switch mode operation, three types of semiconductor components are mainly used:

1. GTO (Gate Turn-Off) thyristors,

2. IGBT (Insulated Gate Bipolar Transistors),
3. IGCT (Integrated Gate Commutated Thyristors).

One of the main characteristics in the selection process of semiconductor devices is the dependence of the locking voltage on the level of the converter input voltage (Table 3.2).

*Table 3.2 Dependence between the standard input voltage values and the required locking abilities of semiconductor devices*

Supply voltage, V	Input voltage or intermediate loop voltage, V	Locking ability of semiconductor devices, V
DC		
750	750 (standard) 900 (maximum)	1700
1500	1500 (standard) 1800 (maximum)	3300
3000	3000 (standard) 3600 (maximum)	6500
AC		
15 000 25 000	1800 (intermediate loop)	3300

Further, these three kinds of semiconductor components will be considered in detail and the most suitable one will be selected.

The main characteristics of the locking thyristors and IGBTs are compared in Table 3.3. The updated GTO variant called the locking thyristor that has an integrated control unit (IGCT) is represented in the table. The main difference between this electronic device and the standard locking thyristor represents the case building and the gate control method supported by the specific control unit (driver). To switch off the upgraded locking thyristor IGCT, the gate current is required equal to the load current. This concept is called «hard control» [JACK03].

Table 3.3 Comparative characteristics of the GTO, IGCT, and IGBTs

Characteristics	IGBT	Locking thyristor		Advantages of IGBT
		GTO	IGCT	
Gating circuit	Voltage controlled	Current controlled	Current controlled	Reduced cost, reliability increase
	$U_{GE} = \pm 15 \text{ B}$	$I_{G_{\text{вкл}}} = 10 \text{ A};$ $I_{G_{\text{выкл}}} \cong 0.3 I_{\text{нагр}}$	$I_{G_{\text{вкл}}} = 10 \text{ A};$ $I_{G_{\text{выкл}}} \cong I_{\text{нагр}}$	
Short circuit protection	Possible for different short circuits	Impossible		Reduced maintenance cost
Current overloading	Possible crystal parallel connection to increase overload ability	Silicon plate diameter: 85 mm		Simplicity of energetic parameters change according to the requirements set
Insulation	Internal	External		Simple construction of module case and simple assembling
Electrical terminals	Internal — sold wire; external — clipped with usual screws	Presses		Simplicity of technical maintenance, easy assembling
Snubber circuit	Not required	Required for switching on and off	Required for switching on	Excluding of snubber circuit simplifies assembling and drops expenses
Switch frequency (standard value), Hz	600	200 – 350		Reduced level of loss radiation, increased efficiency

The data given above show that conduction characteristics and commutation ability make IGBT an ideal electronic switch for the power electrical circuits.

It is expected further to improve of the switch characteristics and direct volt-ampere characteristics of IGBT. Nevertheless, in the nearest ten years no jumps in the power semiconductor technique is predicted. With IGBT implementation, the period of fast change finished by the replacement of usual thyristors by IGBTs, which affected the traction converter development. The new semiconductor materials, like the silicon carbide (SiC), have a long way to go before their implementation into the mass production technology for the devices, the power of which reaches the level of traction power converters.

### **3.2.2 Method for IGBT calculation**

The problem of switch selection is one of the critical problems in upgrading a tram. It is quite difficult to find any common and complex decisions due to the specifics of each project. Though the solutions differ significantly, still their starting position is invariable concerning the full matching to the load. In terms of loading it is required to, develop an algorithm for the IGBT selection in the tram update process.

First, transistor parameters are selected for the traction drive system where the motor control is concentrated on a single converter. As a motor, the ATR200L family of Slovres AS Company was selected. The main data of IGBTs are:

1. voltage,
2. current flow possibilities under appropriate cooling conditions and commutation frequency,
3. safe operation area.

In the case of standard static and dynamic operational conditions, the locked voltage, pulse current, and junction temperature did not exceed the safe operation area.

An analysis of the direct locked voltage takes into account the no-load level 540 - 621 VDC and the line-to-phase level in the input of the converter substation in the range of 400 - 460 V, while the B6 rectifier is used. In this case, the IGBT locked voltage of 1200 V may be referred. For B6 rectifiers, 1700 V is selected assuming 20 % overvoltage per an individual stage [SEMI04].

To find the parameters of the tram drive, an approach suggested by [SEMI04] was applied to the case when each of the two motor pairs is supplied by its own inverter. Then,

1. forward locked voltage that satisfies the mains parameters is equal to 1200 V,
2. forward current  $I_c$  with a 20% reserve is 305 A (400 A),
3. resistance  $R_{thjc}$  is  $0,064 \Omega^{\circ}C$  and saturation voltage  $V_{Cesat}$  is 4 V,
4. effective current in overloading is in the range  $1,9 \dots 2,2 I_n$ ,
5. commutation frequency does not exceed 20 kHz.

In the third combination of the traction frequency converter for the tram assume that

1. forward locked voltage that satisfies the mains parameters is equal to 1200 V,
2. forward current  $I_c$  with 20% reserve is 153 A (200 A),
3. resistance  $R_{thjc}$  is  $0,12 \Omega^{\circ}C$  and saturation voltage  $V_{Cesat}$  is 4,1 V,
4. effective current in overloading is in the range  $1,9 \dots 2,2 I_n$ ,
5. commutation frequency does not exceed 20 kHz.

Further, the IGBT module selection may be processed based on the obtained parameters of each drive combination for KT – 4 trams.

IGBTs are manufactured by a number of companies, the most popular of which are SEMIKRON, ABB, FUJI, HITACHI, etc.

### **3.2.3 Algorithm Selection for the Traction Converter Switch Control**

The algorithm of the inverter switch control serves for the required voltage and current programming. Today, a great number of methods have been developed to commute the three-phase voltage inverter switches. As a rule, they may be divided into two groups:

1. all switches are commutated simultaneously,
2. switch groups are commutated according to the preselected inverter states.

In the first group, the pulse-width modulation (PWM) is presented. A number of PWM methods are known. Among those are the following:

1. basic PWM assumes the command sinusoidal signal and the carrier signal of the saw-toothed or triangle waveform, which defines the commutation frequency of the inverter switches to be compared;
2. modified PWM assumes an increased output voltage thanks to the non-sinusoidal command signals obtained by pre-modulation;

3. optimum PWM assumes improved harmonic contents of the output voltage thanks to the specific model of the commutation time calculation;
4. hysteresis current PWM (so-called “current corridor”) assumes switching time calculation using the comparison of the referred and the actual currents in the specific comparator.

The second group includes the methods based on the space vector theory. Each switching group switches on here in accordance with the definite space position of the voltage vector applied to a motor. These methods are defined in conformity with a three-phase autonomous inverter as

1. basic control methods,
2. vectorial PWM.

Vectorial PWM is the most appropriate control algorithm for the traction converter switches having an autonomous inverter topology. This algorithm provides the same maximum output voltage as the modified PWM, thus allowing more complete mains voltage usage though a majority of produced DSPs imply vectorial PWM, including the DSP TMX320F2812, which has been suggested for the control system of a traction drive [LEO01], [IIIPE00].

Since the maximum output voltage is known, the rated voltage of the traction motor can be defined. It is assumed that the motor consumes full mains voltage in the rated mode. The motor rated voltage is an effective phase-to-neutral voltage value. Thus, the rated voltage may be calculated using the formula

$$U_{nom} = \frac{u_d \cdot \sqrt{3}}{\sqrt{3} \cdot \sqrt{2}} = \frac{u_d}{\sqrt{2}} \quad (3.1)$$

where  $u_d$  – mains voltage, which serves as the output inverter voltage, V.

Mains voltage is equal to  $600 \pm 200$  V. To define the rated voltage of the traction motor, 600 V is assumed as the desired value, because the less voltage is required when the rotational speeds do not reach the rated ones. Since the rotational speed exceeds the rated value, an undervoltage will limit the tram acceleration in the given speed range. The steady-state motion velocity is slightly affected by this voltage, because the resistance force is of minor importance, as the traction calculation shows.

Rated voltage, V

$$U_{nom} = \frac{600}{\sqrt{2}} = 424 \quad (3.2)$$

This result is displayed in Table 2.12, where the main required characteristics of the traction motor are collected for the upgraded tram.

The choice of the inverter commutation frequency is of major importance for any kind of PWM. Increased inverter commutation frequency provides the following advantages:

1. increase in the dynamic accuracy of the command torque and speed reproduction;
2. increase in the motor drive frequency midband;
3. decrease in the amplitudes of the modulation current ripples, magnetic flux and torque, as well as the reduction of modulation loss;
4. motor produced noise reduction.

At the same time, an increase in the commutation frequency leads to some negative consequences:

1. increase in the commutation frequency leads to an increase in inverter commutation losses, thus lowering the inverter output capacity;
2. capacitive currents grow in the supply cables and motor constructional elements, thus extending the losses in the “autonomous inverter – induction motor” system;
3. the problem is complicated in terms of the overvoltage limitation caused by the stray waves in the load chain as well as the decrease of the voltage degree of use in the converter elements.

Decrease of commutation frequency leads to the inverse consequence. Thus, the goal of the commutation frequency selection for the traction converter is to obtain the maximum efficiency in the “autonomous inverter – induction motor” system taking into account the required fast response and voltage necessary level restriction. Torque ripples do not play any significant role because they cannot cause the pulsation in the tram wheel speed thanks to the high moment of inertia of the traction drive as well as the almost sinusoidal output voltage waveform.

### **3.3 Design of the input LC filter for the power converter**

#### **3.3.1 Mathematical model of the input LC filter**

The input filter is calculated for the model inverter of the traction drive with a dc link and the control algorithm based on the vectorial PWM [MOH95]. The dc link current is assumed as

$$I_d = \frac{3 \cdot U_{\text{инв,вых}} \cdot I_{\text{инв,вых}}}{U_d} \cdot \cos \varphi = \frac{3 \cdot U_d \cdot I_{\text{инв,вых}}}{\sqrt{3} \cdot \sqrt{2} \cdot U_d} \cdot \cos \varphi = \frac{\sqrt{3}}{\sqrt{2}} \cdot I_{\text{инв,вых}} \cdot \cos \varphi \quad (3.3)$$

where

$I_d$  – dc link current, A,

$U_d$  – inverter input dc voltage, V,

$U_{\text{инв,вых}}$  – effective value of the inverter output voltage, V,

$$(U_{\text{инв,вых}} = \frac{U_d}{\sqrt{3} \cdot \sqrt{2}})$$

$I_{\text{инв,вых}}$  – effective value of the inverter output current, A (defined by the load)

$\varphi$  – angle between the fundamental harmonics of the inverter output current and voltage.

The capacity of the input capacitor required to compensate reactive power is defined as [САРЕ80]:

$$C_{\text{ex}} = \frac{\int_t^{t+\Delta t} i_d dt}{\Delta U_c} \quad (3.4)$$

where

$\Delta t$  – time slot while the current flows from the inverter to the source,

$\Delta U_c$  – possible overvoltage on the capacitor.

Based on the given formula solution, the capacitance is as follows:

$$C_{\text{ex}} = \sqrt{\frac{\sqrt{3}}{2}} \cdot \frac{\mu \cdot \sqrt{2} \cdot I_{\text{инв,вых}}}{f_k \cdot \Delta U_c} \cdot \sin^2 \frac{\varphi - \pi/6}{2} \quad (3.4)$$

where

$f_k$  – commutation frequency, Hz,

$\mu$  – modulation factor.

To define the input capacitor value, the base mode is assumed under the motor no loading on the rated rotational frequency because of the maximum angle  $\varphi$  in this mode. Induction motor of 1,5 kW capacity has the no-load

current close to 50 % of the rated value and  $\cos\varphi$  near 0,1. Inverter commutation frequency is assumed 5000 Hz. Capacitor overvoltage is assumed equal to one percent of the rated value, i.e. 6 V. Then, the input capacitor value is

$$C_{\text{сблх}} = \sqrt{\frac{\sqrt{3}}{2} \cdot \frac{\sqrt{2} \cdot 3,2}{5000 \cdot 6} \cdot \sin^2 \frac{84 - 30}{2}} = 29 \mu F \quad (3.5)$$

The input capacitor value must correspond to the smoothing conditions for the input voltage. The source of the model inverter dc voltage is the controlled thyristor rectifier, built as the bridge. In [ПУД80], to define the capacity of the input capacitor the following expression is used:

$$C_{\text{сх}} = \frac{I_d}{m_n \cdot \omega_c \cdot U_{\text{пульс}}} \quad (3.6)$$

where

$m_n$  – pulse number of the rectified voltage in the supply voltage period,

$\omega_c$  – angular frequency of the supply voltage, Hz

$U_n$  – required amplitude of the input voltage ripple, V

To calculate the capacity, the required maximum current of the dc link is equal, A

$$I_d = \frac{\sqrt{3}}{\sqrt{2}} \cdot 12,8 \cdot 0,8 = 12,5 \quad (3.7)$$

In the dc link calculation, the maximum motor current is twice more than the rated value.

Assuming the output voltage ripple as 30 V (5% of rated value), define the necessary capacitance of the input capacitor,  $\mu F$ , was defined using the formula:

$$C_{\text{сх}} = \frac{12,5}{6 \cdot 314 \cdot 30} = 221 \quad (3.8)$$

The fundamental harmonic of the three-phase bridge rectifier ripple has the frequency which exceeds the mains frequency six times. During the choke inductance selection of an LC filter, the resonant frequency is assumed close to 50 Hz [ШЕ85]. Then, the needed choke inductance equals, mH,

$$L_{op} = \frac{1}{4 \cdot \pi^2 \cdot f_{cp}^2 \cdot C_{ex}} \quad (3.9)$$

where

$L_{op}$  – choke inductance, mH,

$f_{cp}$  – cutoff frequency, Hz.

To calculate the choke, the input capacitor capacity is assumed from the condition of the rectified voltage ripple smoothing, i.e. 221  $\mu$ F. Then, the required choke inductance, mH, is

$$L_{op} = \frac{1}{4 \cdot 9,87 \cdot 2500 \cdot 0,000221} = 46 \quad (3.10)$$

The choke having an inductance 46 mH will be of high size and cost thus it is advisable to assume less inductance than with calculated one, in order 10 mH for the traction drive inverter. In this case, the capacity required for the cutoff frequency 50 Hz will be, in  $\mu$ F

$$C_{ex} = \frac{1}{4 \cdot 9,87 \cdot 2500 \cdot 0,01} = 1000 \quad (3.11)$$

To obtain such capacity on the rated voltage 600 V, two series connected capacitors may be used, each of 2000  $\mu$ F.

### 3.3.2 Variants of input filters

There are some techniques to calculate an input filter for the tram inverter:

1. common input filter for n inverters,
2. common input filter for two inverters,
3. input filter for each of four inverters.

Each technique was examined sequentially [ШЕИФ85].

### 3.3.3 Calculation of the input filter for N inverters

First, assume that the common inverter controls four induction motors. Use a motor of ATR200L - 4 series from Slovres AS Company.

To calculate an input capacitor in the operation mode, the formula (3.12) was used:

$$C_{ex} = \sqrt{\frac{\sqrt{3}}{2}} \cdot \frac{\mu \cdot \sqrt{2} \cdot I_{инв,вых}}{f_k \cdot \Delta U_C} \cdot \sin^2 \frac{\varphi - \pi/6}{2}, \quad (3.12)$$

where

$f_k$  – commutation frequency, Hz,

$\mu$  – modulation factor,

$I_{\text{инв,вых}}$  – effective value of inverter output current, A,

$\varphi$  – angle between the fundamental harmonics of the inverter output current and voltage,

$\Delta U_C$  – permissible overvoltage on the capacitor.

Assume the commutation frequency as 4000 Hz, inverter output current as 508 A, and permissible overvoltage as 6 (1% of supply voltage).

Using (3.12) obtain  $C_{\text{вх}} = 0,00266$  F.

A transformer sub-station produces the output voltage, of the level constancy which is not guaranteed. Thus, the input filter has to meet the requirements of the input voltage smoothing. To calculate the smoothing capacitor that protects from the supply voltage influence, formula (3.13) was used.

$$C_{\text{ex}} = \frac{I_d}{m_n \cdot \omega_c \cdot U_{\text{нульс}}}, \quad (3.13)$$

where

$m_n$  – pulse number of the rectified voltage in the supply voltage period,

$\omega_c$  – angular frequency of the supply mains voltage, Hz,

$U_n$  – required amplitude of the output voltage ripple, V,

$I_d$  – dc link current, A.

Supply voltage frequency meets the frequency of the input power transformer being equal to 50 Hz. Pulse number equals 6. Ripple amplitude is assumed 5% of the mains voltage and equals 30 V.

DC link current was calculated using the equation (3.14).

$$I_d = \frac{3 \cdot U_{\text{инв,вых}} \cdot I_{\text{инв,вых}} \cdot \cos \varphi}{U_d} = \frac{3 \cdot U_d \cdot I_{\text{инв,вых}} \cdot \cos \varphi}{\sqrt{3} \cdot \sqrt{2} \cdot U_d} = \frac{\sqrt{3}}{\sqrt{2}} \cdot I_{\text{инв,вых}} \cdot \cos \varphi, \quad (3.14)$$

where

$U_d$  – inverter input dc voltage, V,

$I_d$  – dc link current, A,

$U_{\text{ИИБ,ВЫХ}}$  – effective value of the inverter output voltage, V,

$\varphi$  – angle between the fundamental harmonics of the inverter output current and voltage,

$I_{\text{ИИБ,ВЫХ}}$  – effective value of inverter output current, A

Using Eq. (3.14),  $I_d = 566$  A was obtained.

Further, based on Eq. (3.13),  $C_{\text{BX}} = 0.01$  F was obtained.

On the next step, the inductance of the smoothing choke using Eq. (3.15) was calculated.

$$L_{\text{оп}} = \frac{1}{4 \cdot \pi^2 \cdot f_{\text{cp}}^2 \cdot C_{\text{BX}}}, \quad (3.15)$$

where

$L_{\text{оп}}$  – choke inductance, mH,

$f_{\text{cp}}$  – cutoff frequency, Hz equal 50 Hz,

$C_{\text{BX}}$  – input capacitor value,  $\mu\text{F}$ , calculated using (3.13).

In this case, using Eq. (3.15),  $L_{\text{оп}} = 0,00102$  H was obtained.

### 3.3.4 Calculation of the input filter for two inverters

To find the parameters of the input filter for the two inverter supply, assume that the load consists of four induction motors ATR200L – 4, where the first inverter controls the first pair whereas the second inverter controls the second pair of the tram bogie motors. Then, by the calculation using the formulas in Section 3.3.3, new results will be obtained for each of the two inverters.

According to Eq. (3.12),  $C_{\text{BX}} = 0,00133$  F or 1,33  $\mu\text{F}$  was obtained.

The expression (3.14) gave  $I_d = 283$  A.

Then, using Eq. (3.13), the capacity to smooth the supply voltage  $C_{\text{BX}} = 0,00501$  F was obtained.

Finally, from Eq. (3.15),  $L_{\text{оп}} = 0,00204$  H was found.

### 3.3.5 Calculation of the input filter for four inverters

In this case, each inverter controls its own induction motor of ATR200L – 4 family. By calculating this filter using the method described in Section 3.3.3, the following results were obtained according to the Eq. (3.12)  $C_{\text{BX}} = 0,00066$  F or 0,66  $\mu\text{F}$ , according to Eq. (3.14)  $I_d = 142$  A. Further, from Eq. (3.13), the capacity to smooth the supply voltage  $C_{\text{BX}} = 0,00251$  F was obtained. Finally, from Eq. (3.15),  $L_{\text{оп}} = 0,00407$  H was found.

The final data are collected in Table 3.4.

*Table 3.4 Dependence of the input filter parameters on the inverter configuration*

Quantity \ Variant	1	2	4
Inverter input capacity ( $\mu\text{F}$ )	2,66	1,33	0,66
DC link current (A)	566	283	142
Supply voltage smoothing capacity ( $\mu\text{F}$ )	10	5,01	2,51
Smoothing inductance (mH)	1,02	2,04	4,07

As follows from the table, the higher the inverter motoring load decreases, the higher the current, supply capacitance and inverter input capacitance decrease, though the input inductance grows.

### **3.4 Conclusions**

In Chapter 3, different problems concerning the design of the TAMM frequency converters were raised and solutions provided.

1. The comparative analysis of the control structures for the TAMM frequency converters was carried out. The analysis made it clear that the vector control is the optimum control method of contemporary traction drive.
2. A decision in favor of the classic vector control was made as a result of the comparison of the classic control and direct torque control (DTC).
3. Vector control algorithms were developed for the group of parallel-connected induction traction motors. Using the MATLAB toolbox, the comparative analysis of the methods was made. As a result, the most optimal method was selected.
4. The method of the input LC filter design for the power converter is suggested. The calculation algorithms were developed and tested for the two, four, and N inverter calculation.

## **4 COMPUTER SIMULATION AND EXPERIMENTAL RESEARCH OF MOTOR DRIVE COMPONENTS**

### **4.1 Computer simulation**

Computer simulation helps to conceive a drive operation prior its desig. Below, a laboratory drive setup is simulated. The possibility to experiment with the calculated data in the laboratory setup measurements provides a basis to apply the same simulation method to the real full-size drive.

#### **4.1.1 Control system model**

To control the inverter, the vector PWM module (Space Vector PWM Control) from the PSCAD soft tool was used. Figure 4.1 shows the model circuit diagram. Here, the variable voltage source is used as the supply source with the inner resistance  $R_{int}=0,01 \Omega$ .  $C$  – is given in  $\mu\text{F}$ ,  $L$  – in H, and  $R$  – in  $\Omega$ .

The calculation step of the simulation is selected as  $t_s = 20 \mu\text{s}$ , that is 1/10 of the period for the frequency 5 kHz. This allows sufficiently accurate representation of circuit processes with required speed of calculation.

Any attempt to decrease the step leads to an increase in the calculation time. Thus, step lowering is unsuitable because quite a long motor running process is to be estimated under the minimum calculation time of some seconds. Step decrease may be excused only when the fast commutation processes are examined in the inverter transistors, taking into account the RC snubber parameters.

### Inverter control

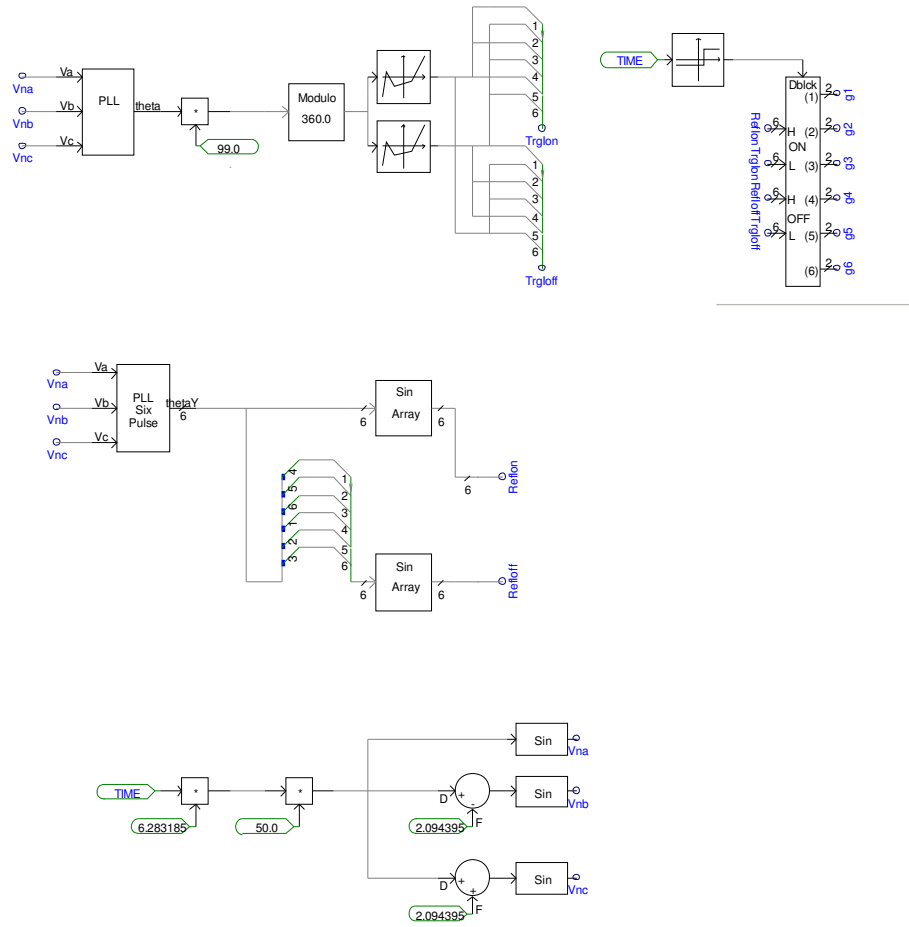


Fig. 4.1 The circuit of the used vector PWM module

### 4.1.2 Simulated processes and result analysis

In this study, main focus is on:

1. charging of the dc link 1000  $\mu$ F capacitor supplied by the mains 1x220 V,
2. charging of the dc link 1000  $\mu$ F capacitor supplied by the mains 3x380 V,
3. inverter running of the 550 W motor supplied by the mains 1x220 V,
4. inverter running of the 550 W motor supplied by the mains 3x380 V,
5. inverter running of the two 2,2 kW motors supplied by the mains 3x380 V.

These processes were studied on the computer model in the hardest conditions, such as the capacitor charging by the direct switching-on without the current-limiting resistor as well as running under the maximum voltage. Diagrams and simulation results are given in the full thesis edition.

## 4.2 Development of the tamd control system elements

### 4.2.1 Development of the control method for induction motor field weakening

Motor operation on the speeds above the rated level serves as the necessary requirement of the traction drive. Nevertheless, some difficulties are connected with the mode. An inverter is unable to generate the voltage that has an amplitude higher than the rated value. This means that due to the constant voltage, further increase of the angular speed is possible in the weakening-field mode only. The ratio between the supply voltage and the angular speed decreases leading to the flux lowering. Accordingly, the maximum torque drops proportionally to the square of the flux reduction [MOR97].

To implement the operation in the field-weakening area using the vector control, the command flux in the controller input must be diminished. When the speeds exceed the rated value, the field weakening is described by the formula: [BON00]

$$\varphi^* = \varphi * \frac{\omega_{nom}}{\omega_{meh}} \quad (4.1)$$

where:

$\varphi$  - rated flux

$\omega_{nom}$  - rated motor speed

$\omega_{meh}$  - mechanical motor speed

Flux curves in different adjustment ranges are displayed by Fig. 4.2.

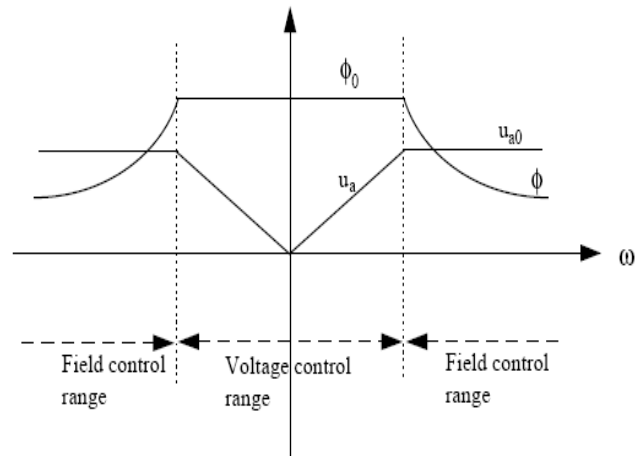


Fig. 4.2 Flux curves in different adjustment ranges

The block diagram that solves the static field-weakening problem in the Simulink toolbox is given in Fig. 4.3. Depending on the current speed, the switching unit passes either the constant rated motor flux or the flux calculated by Eq. (4.1) to the controller input. The unit threshold is set in 154 rad/s, which corresponds to the rated speed.

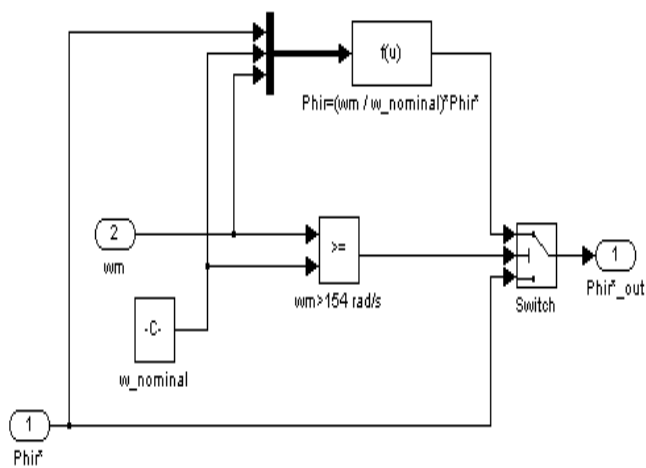
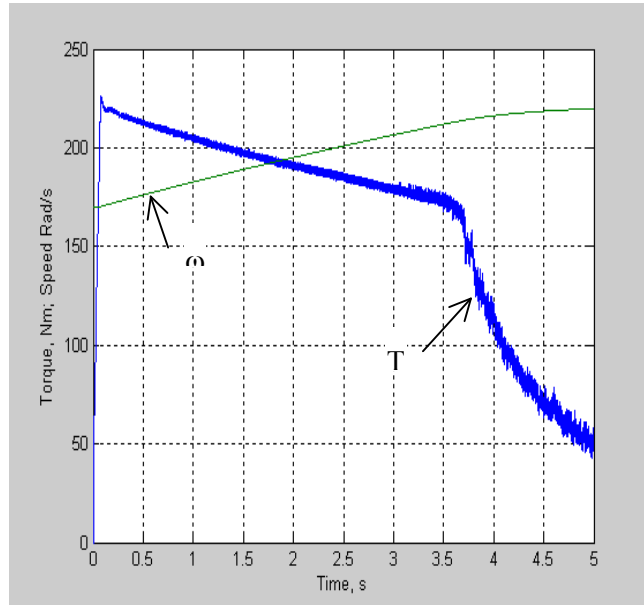


Fig. 4.3 The circuit to solve the static field-weakening problem

The curves in Figs. 4.4, 4.5, and 4.6 show the simulation results. Figure 4.4 represents the motor operation at the rated voltage, Fig. 4.5 shows the operation with the field-weakening unit at the rated voltage, and Fig. 4.6 displays the situation where the supply voltage drops from 780 to 514 V in 0,3 s after the beginning of the simulation.



*Fig. 4.4 Motor operation without field weakening*

As Fig. 4.4 shows, since the motor reaches the speed range 210 rad/s, the supply voltage becomes insufficient and the torque curve drops abruptly. This confirms again the requirement for field weakening.

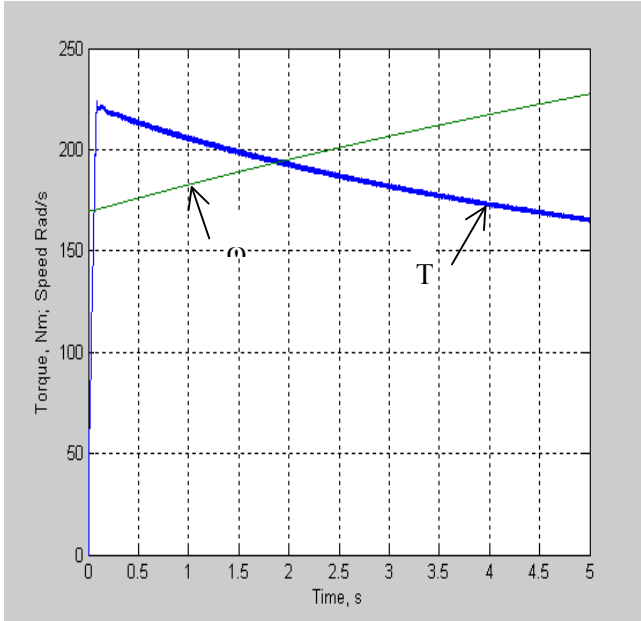


*Fig. 4.5 The field-weakening unit switch-on at the rated voltage*

To weaken the field in the steady-state mode using Eq. (4.1), fine dynamic results may be obtained until the speed exceeds the rated value twice, as demonstrated in Fig. 4.5. Nevertheless, the static field weakening is insufficient at the undervoltage, thus the system has lost the motor control (Fig. 4.5).

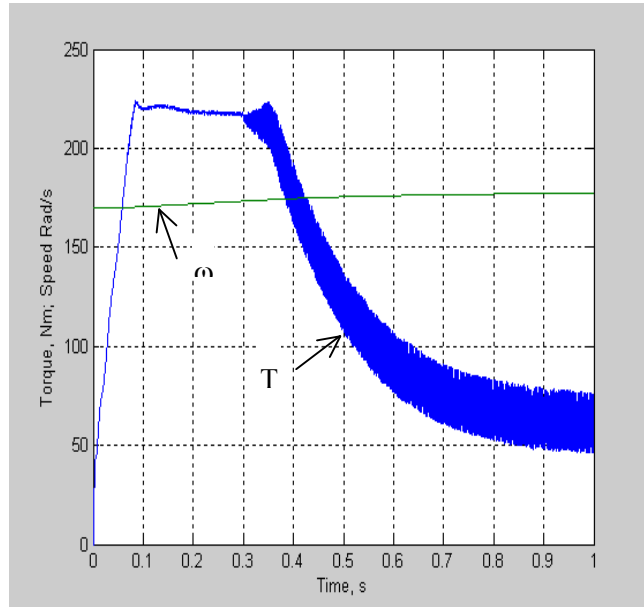


Fig. 4.6 Mains voltage drop from 780 to 514 V

As Fig. 4.6 shows, the static field weakening does not operate at undervoltage. Research of the voltage in the tram supply net shows that the level is not constant changing in the range  $\pm 30\%$  of the rated value. Difficulties in the drive control may occur in the case of sharp voltage drop in the mains. To continue normal motor operation, deeper field weakening is required in addition to the static weakening, with regard to the possible voltage level.

To solve the problem of deeper field weakening, a dynamic field-weakening system is suggested. The system enables the maximum possible magnetizing current value to be supported at any supply voltage that, in turn, allows for the development of the maximum possible torque on the motor shaft. Figure 4.7 represents the dynamic field-weakening unit.

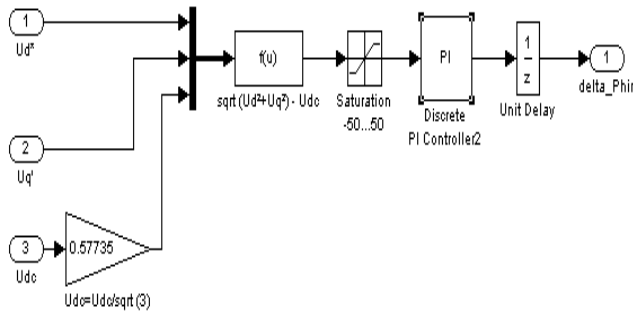


Fig.. 4.7 Dynamic field-weakening unit

If the voltage control vector exceeds the permissible value, the referenced motor flux decreases using the circuit built on the PI controller. The minimum flux is restricted by 10% of the rated value. The simulation result of the dynamic field weakening is shown in Fig. 4.8. The conditions and the time of the voltage drop are the same as in Fig. 4.6.

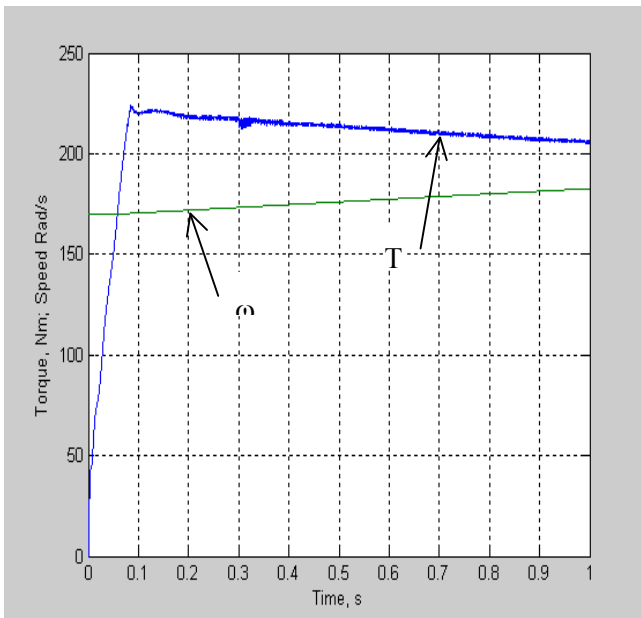


Fig. 4.8 Result of the operation of the dynamic field-weakening unit

The simulation shows visually an efficiency of the suggested field-weakening method. Note also that with field weakening, it is required to decrease the torque-developing component of the current simultaneously because an unlimited field weakening is impossible. Unlike the first method,

the dynamic field-weakening response time is limited; therefore, some torque pulsation is noticeable in the diagram.

#### **4.2.2 Development of the speed measuring device for the induction motor**

Different speed sensors convert the motor's angular speed or the motion velocity of the mechanism's executive device into the electrical signal. Tacho generators as the dc and ac micro machines are widely used speed sensors. However, the tacho's accuracy may be insufficient for contemporary automatic motor drive systems that have a wide speed adjusting range and high stability requirements. The digital speed sensors are introduced into such systems [TEP87].

In the sensor selection, the first step is to define the right priorities based on the following criteria:

1. resolution and accuracy,
2. linearity,
3. speed of measuring process,
4. operational conditions and protection class,
5. reliability,
6. frame size,
7. cost.

Using the above-mentioned criteria, the pulse speed sensor GI328 was selected. The sensor has a number of advantages, such as high resolution, reaching 2048 pulses per revolution, small size, speed up to 12000 rev/s, and direct interface with the microprocessor [БОЙ04].

In the drive laboratory setup, the microprocessor TMS320F2812 of Texas Instruments was used. The processor allows two variants of the digital code generation to be studied. For this, the so-called "event manager" was built into the processor. To calculate the time interval between the pulses, both the speed sensor channel having 2048 pulses per revolution and the mixed two-channel signal that gives 4096 pulses per revolution may be used. Each new pulse causes the "event manager" to fill the stack by the speed timer (150 MHz) value. Then, the actual speed is calculated using the difference of the calculated time codes.

The specific unit "Quadrature Encoder" could also be used, the operation of which is explained in Fig. 4.9. Sensor signals QEP1 and QEP2 enter the input of the unit. Fourfold frequency Quadrature CLK and the rotational

direction signal are presented in the output. The counter calculates pulses per definite time depending on the rotational direction [TIEV02].

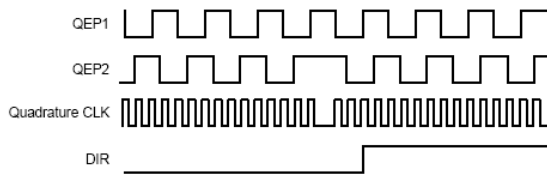


Fig. 4.9 Operation principle of the “Quadrature Encoder“ unit

First, an error is calculated caused by the discreteness of the speed sensor inquiry. It depends on the transient speed and reading frequency. The reading frequency is limited by the execution speed of the vector control algorithm, which is 5000 Hz in the laboratory setup.

The smaller the reading frequency, the higher an error may be. Fig. 4.10 represents error dependence on the reading frequency.

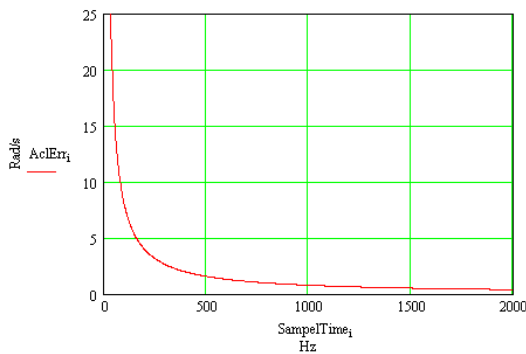


Fig. 4.10 Error versus the reading frequency

In the pulse-to-pulse time interval calculation, some problems occur. This method does not allow the rotational direction to be defined. The frequency of the updating speed data is variable and depends on the speed. When the speeds are very low, the number of base pulses reaches infinity. The processor counter calculates up to 65536 pulses, thus the actual minimum speed is approximately equal to 1,5 rad/s. In the case of the base pulse frequency decreasing, the high-speed resolution drops (Fig. 4.11).

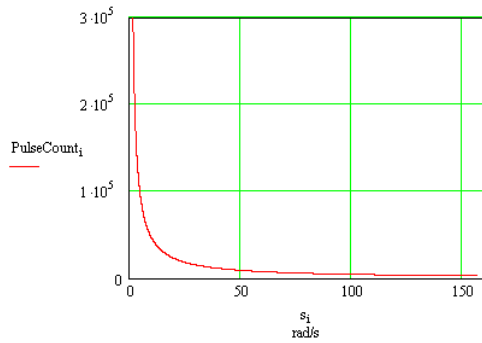


Fig. 4.11 The number of base pulses versus angular speed

Another method allows the rotational direction to be defined in addition to the speed value. Obtaining the actual speed data may be synchronized here with the calculation algorithm. From now on, an error can be calculated, resulting from the finite number of pulses coming from the sensor in the time unit. The full error is the sum of the reading error and the finite pulse number error. Figure 4.12 gives the sum of the speed measuring errors.

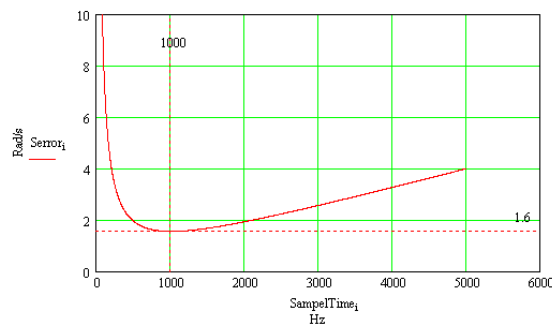


Fig. 4.12 Speed measuring error versus the reading frequency

The summary error reaches its maximum at the reading frequency of 1000 Hz being equal to 1,6 rad/s. It is ~ 1 % of the rated motor rotational speed.

Because of the described research and calculations of the measuring accuracy, the calculation method of the pulse number per time interval was selected. Its implementation gives a number of advantages: the possibility of direction the rotational, constant high measurement accuracy at different speeds, and suitable synchronization with the control algorithm cycle. Thanks to the built-in decoder of the processor, this method is simple in implementation.

### **4.2.3 Analysis of solutions to the TAMD electromagnetic compatibility problem**

Pulse-width modulation (PWM) used in the inverters is the source of different high harmonic noises in addition to the fundamental harmonic.

High harmonics penetrate into the measurement loops of the control system, deteriorating the overall control system operation. Following the high-order harmonics, the noise occurs in the voltage measurement, which diminishes the possible gains of current controllers, drive dynamics, and common system stability. Low-order harmonics worsen the parameters of the vector control system, causing torque shocks in the motor [SEU00].

Fast change of the voltage and current of electronic devices results in electronic noise from both emission and induction. The basic noise exists in the power transistors switching-on and off.

Dynamic changing currents lead to the variable magnetic fields, the screening of which screening is more difficult than in the case of electrical fields. A changing magnetic field may carry the currents in other circuit chain,s resulting in a new noise [BAR01].

In an electromagnetic emission (EMI) analysis, three factors must be examined:

1. EMI source (generator),
2. emission transfer paths,
3. emission consumer (victim circuit).

It is remarkable that the defense of EMI requires a systematic approach. Receiver improvement does not bring success while the EMI source force is high. Thus, minimization of the source emission is the first step, whereas the conductivity of the transmission paths and the receiver sensitivity decreasing are the next steps. The last consideration is very important because usually the receiver serves as an EMI relay.

EMI screening occurs because a metal of good conductivity decreases the emitted electrical field by the wave reflection and absorption being placed between the EMI source and the protected circuit.

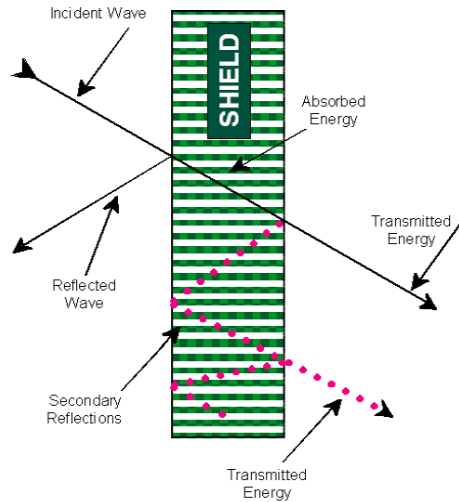


*Fig. 4.13 EMI weakening by the conducting screen*

The type (reflection or absorption) and weakening degree depend on the factors: frequency, emission wavelength, the metal conductivity and passability, and its distance from the source. At high frequencies, screen width does not play any role [NORM04].

Metallic plates also serve as screens against magnetic fields but they are the screens of other kind. Non-ferromagnetic metals do not affect magnetic fields, having the frequency below 10 MHz. Aluminum is practically transparent for these kinds of fields. To pass a magnetic field, a material is to be ferromagnetic and to have low magnetic resistance [HILL04].

Noise drop in the signal circuits may be obtained by the use of screening cables and ferrite rings, which both the wires and the screen pass through. As a rule, screen grounding from the noise side is required, thus avoiding the problem of noise return to the source through the ground [FRAN01].

The screening of signal converter boards can be provided by metal plates. The signal converter is not screened from the supply wire because this wire passes via the sensor itself.

One reason of noise is poor grounding (Fig. 4.14).

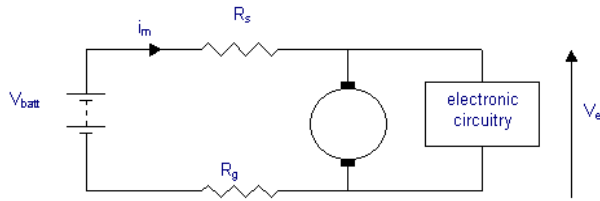


Fig. 4.14 Typical circuit with common grounding

As the circuit shows, the supply wire and the «earth» wire have common resistances  $R_s$  and  $R_g$ . While the current flows, these resistances cause the voltage drops  $i_m R_s$  and  $i_m R_g$ , which lead to the voltage drop in electronics with  $V_{batt}$  by  $i_m(R_s + R_g)$ . The current switching on and off due to the motor collector will cause voltage drops in the electronic supply. To solve the problem, it is reasonable to insulate electronic circuits from the power supply, providing the separated electronic supply (Fig. 4.15). An example is the DC-DC converter, which provides the insulated supply from the existing source. All grounding loops must have minimum resistance.

Another example of galvanical disconnection is a current sensor built on the Hall effect. This sensor provides an overall insulation of power circuits from the measuring circuits.

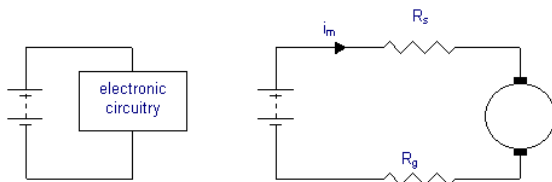


Fig. 4.15 The circuit with split supply

Usually, the snubber consists of the resistor and capacitor that rounds the voltage ripple source or the protected circuit (Fig. 4.16). Possibly, both loops may be used simultaneously.

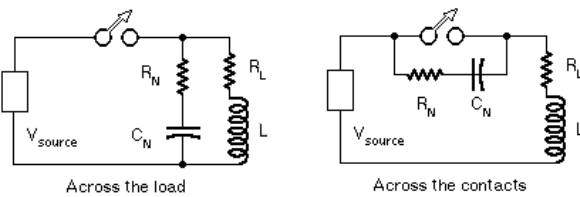


Fig. 4.16 Examples of a snubber

The main function of the snubber relates to the noise energy absorption. in According to the energy consumption type, snubbers are divided into two

types, either that of voltage or current. The capacitor across other circuit components controls the voltage. The inductor adjusts the current.

Snubbers improve and increase commutation circuit efficiency, allowing frequency rise and EMI drop.

To protect the measuring signals from noise, analog and digital filters or their combination may be used. By using the analog low-pass filter, the low-frequency noise is deleted before the analog-to-digital conversion (ADC). Accordingly, the digital data of ADC do not include unnecessary harmonics (Fig. 4.17).

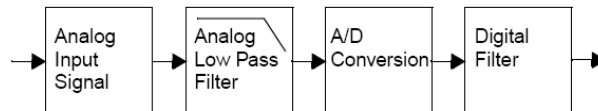


*Fig. 4.17 Data input channel*

In particular, an analog signal includes outside voltage spikes inaccessible to the digital filter that may saturate ADC. This causes errors even if the average signal does not exceed the ADC permissible borders [BONN02].

Digital filtration is one of the strengthened DSP properties thanks to obvious advantages and the absence of the filter drawbacks in terms of the parameter instability of passive elements in time, with temperature, and due to different problems with active components (operational amplifiers, etc.). Digital filters have characteristics unattainable with the analog devices. Moreover, parameters of the digital filter may be corrected easily through the software.

By digital filtration, the filtered signal parameters may be adjusted. It is important to find difference between the amplitude and phase errors of the filtered signal to protect the circuit against them.

The current harmonic content depends on the type of the used PWM. At periodic PWM, unlike the stochastic PWM, the harmonic specter is strictly defined. In the case of sinusoidal PWM and space vector PWM, the first current harmonic has the frequency of the commutation twice and is synchronized with PWM.

While the sensor's reading frequency is twice higher than the commutation frequency and is synchronized with PWM, the main current harmonic is measured without filtering.

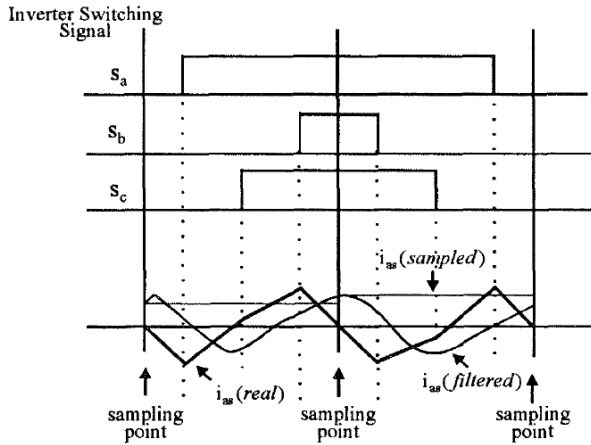


Fig. 4.18 PWM signals, motor current, reading point, filtered and measured current signals

Figure 4.18 shows the PWM signals, motor current, reading point, filtered and measured current signals in typical situation. In real conditions, the low-pass filter cuts the inverter noise. After the signal passes the low-pass filter, the measured current has the amplitude and phase errors. An example is shown in the figure above. While the filter cutoff frequency equals the reading frequency, the measured current is practically equal to the maximum motor current with some phase shift.

To exclude the problem, the reading delay may be beneficial in accordance with the filter delay. Finally, the averaged current value will pass to the output without a phase error.

#### 4.2.4 Development of current measuring tools for the frequency converters

The experimental setup of the traction drive is shown in Fig. 4.19. Further, the use of the above given recommendations in the setup is explained.

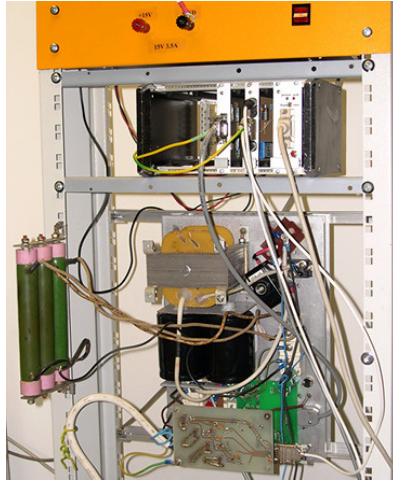


Fig. 4.19 Laboratory setup of the drive

### Sensors

To measure the high frequency current in the inverter, the current sensor LTS 15-NP was selected (Fig. 4.20). The sensors of this type have galvanic decoupling between the measured and measuring circuits. The sensor is intended for the following applications:

1. servomotors and variable-speed drives,
2. static converters for dc motors,
3. uninterruptable supply sources,
4. welding machine suppliers.

Their main technical parameters are given in Table 4.1.

Table 4.1 Technical parameters of LTS 15-NP

Measured current, A	15
Supply ( $\pm 5\%$ ), V	5
Error @ IPN, $T_A = 25^\circ\text{C}$	$\pm 0.2$
Following the change in $di/dt$ , $\text{A}/\mu\text{s}$	35
Frequency range (0 .. -0.5 dB), kHz	DC..100

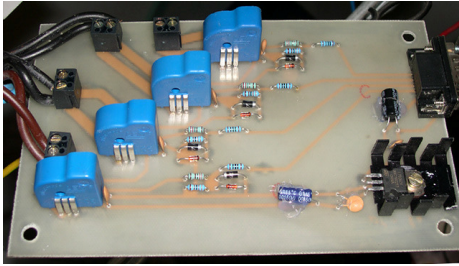


*Fig. 4.20 Current sensors*

### **Sensor supply**

The board for the current sensors is supplied by the galvanic insulated supply unit, 15V.

### **Analog filter**

For the analog filtering, the simplest filter concept was used. To follow the signal interface, the ceramic capacitor of 100 nF was placed between the signal wire and the earth.

### **Screening**

Screened cables were used for signal transfer from the current sensors to the signal processor. The screen was grounded from the noise source side.

### **Snubbers**

Snubbers were used to decrease the voltage spike amplitudes on IGBTs (Fig. 4.21). The capacitor between the inverter positive and negative poles had the ratio 0,47  $\mu$ F/1000V.



*Fig. 4.21 Snubber capacitors*

DSP TMS320F2812B from Texas Instruments was used.

Simulation of the drive operation by the Matlab-Simulink toolbox showed that in the high-frequency noise of the current feedback no such problems occur as with the phase shift of the fundamental harmonic. To decrease the noise and fix the phase, the digital first-order filter was used. It is the so-called filter with the finite pulse response.

The filter output signal is

$$y_i = \frac{f_{i-1} + f_i}{2},$$

where  $f_i$  is the measured signal.

The processor has the built-in PWM signal generator. It allows quick synchronizing of the measured current signals and the PWM signals. The main control cycle was calculated per certain PWM period.

The measured results were obtained on the drive setup built on the motor 2.2 kW. PWM frequency was 5 kHz. The measured current of the first phase is shown in Fig. 4.22.

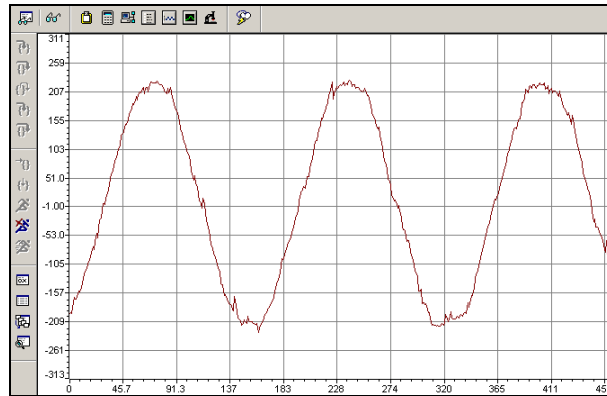


*Fig. 4.22 Calculated current of the first phase*

Comparison of the directly measured and 50 Hz filtered curves shows the phase error near one degree without an amplitude error.

### 4.3 Conclusions

Chapter 4 presents the results of computer simulation and experimental research of the drive components.

1. The computer model of the drive control system was designed for the study of different operation modes.

2. The dc link capacitor modes of charge from the single-phase and three-phase sources were performed resulting in the definition of optimum starting conditions for the single and two motors supplied by different sources.
3. A new field-weakening approach is suggested for the induction motor. In this connection, the two possibilities of such control were examined. The first one concerns the proposed formula for the required motor flux calculation depending on its rated value and actual motor speed. However, this method provides the drive inspection only in case the voltage is equal to the rated one.
4. Next, the method of the dynamic field weakening was designed, which allows soft tuning of the motor flux to obtain its maximum possible value even at undervoltage. However, the flux cannot be decreased infinitely; therefore, the inspection of possible motor torque is required.
5. It is shown that the sequential connection of the two field-weakening units is An advisable. This provides that only one static field-weakening unit operates at the rated voltage level, allowing growth in the drive operation stability.
6. Additionally, two devices were developed: one for the induction motor speed measurement and the other for the frequency converter current measurement. In the latter design, the main sources of electromagnetic emission were examined and a number of techniques were proposed to overcome emission.
7. The use of DSP was suggested to obtain the desired system current quality. Practical results have proved the proposed solution.

## 5 SUMMARY

1. Analyses of the traction drive power circuits and classification of the driving tools are proposed in the thesis.
2. Engineering and economic bases of the expediency of the development and research of the novel motor drive system are provided using the solutions earlier obtained in the Department of Electrical Drives and Power Electronics.
3. Analysis, comparison, and regimentation of the known and prospective principal decisions in the TAMD configurations scope were carried out.
4. Solution to the topology optimization problems and contents of the traction ac drives is provided, including the selection of motor and converter type, control method, and element base.
5. Comparative analysis and selection of the TAMD simulation tools was realized, including the grounding of the required software.
6. In the thesis the induction motor equivalent circuit for the multimotor traction system was developed and defined, including a comparative analysis of obtaining the equivalent circuit parameter methods.
7. The TAMD calculation and motor selection methods were developed and tested, well as the justification in terms of possible replacement of the entity dc motors by the ac ones.
8. A method of the motor drive traction calculation was developed, including the motor and generator modes, and inverter braking resistor.
9. A comparative analysis of the TAMD frequency converter control structures was made, including the proof of the vector control requirement.
10. Development of the vector control algorithms for the group of parallel-connected induction traction motors is included.
11. A comparative analysis of the suggested vector control algorithms is presented, including the selection of an optimum one.
12. The design method of the input LC filter for the power converter and test results of calculation algorithms for two, four, and N inverters are given.
13. A computer model of the motor drive control system was built to study different modes of operation.
14. Technology and results of computer research in the capacitor charge of the dc link supplied by the single-phase and three-phase mains, including the search of optimum conditions for the single and two-motor running having a different supply are discussed.

15. A novel approach to the induction motor control by the field weakening taking into account various possibilities of such adjustment is suggested.
16. A formula to calculate the required motor flux using its rated value and speed is proposed, including the analysis of the product area.
17. A novel method was developed for the dynamic field weakening, which allows the flexible tuning of the motor flux to obtain its maximum value even under the reduced voltage, including the analysis of its product area.
18. A new circuit is proposed for the series connection of the two field-weakening units, which provides the required unit operation under the rated voltage level, thus giving rise to the drive stability.
19. A novel device for the induction motor speed measurement is suggested.
20. A novel device for the frequency converter current measurement was built, which excludes the main sources of electromagnetic emission.
21. A method of the DSP usage to obtain the required system current quality was designed and proved by the practical results of its application.

## 6 REFERENCES

- [BAK02] Bakran, M. M. «Железные дороги мира.» *Применение тяговых преобразователей на базе транзисторов IGBT*. 05 2002 г. <http://www.css-rzd.ru/zdm/05-2002/02084-1.htm>.
- [TTTK06] ТТТК. Историческая справка ТТТК. 2007. <http://www.tttk.ee/union/history/>.
- [ПЕР06] Перепелятник, С. *Современный асинхронный тяговый привод*. 2006.
- [JOL01] Joller, J. *Trammide energiasäästlike veoajamite uurimine ja väljatöötamine*. Thesis of Tallinn Technical University, ISBN 9985592050, Tallinn Technical University Press, 2001
- [INT98] International Railway Journal, 1998, N 10, p. 56.
- [MÜL97] A. Müller-Hellmann. *Eisenbahntechnische Rundschau*, 1997, N 6, S. 333 - 338.
- [SAT98] Y. Sato. *Elektrische Bahnen*, 1998, N 6, S. 173 – 178.
- [САВ00] САВБОВ, В.М., *Высокоскоростной поезд нового поколения "СОКОЛ"*, Железнодорожный транспорт, 2000, No5.
- [СТЕП82] А.Д.Степанов, В.И.Андерс, В.А.Пречисский, Ю.И.Гуселевский; *Электрические передачи переменного тока тепловозов и газотурбовозов*, М.: Транспорт, 1982, 254 с.
- [ТЕХ02] Texas Instruments Incorporated, *TMS320F2810 and TMS320F2812 32-Bit Fixed-Point Flash DSPs*, 2002
- [АВВ05] Внутренний каталог цен компании АВВ, (закрытая информация), 2005
- [RJA05] Рябов, В., *Калькуляция и сравнение вариантов силовых схем электропривода с векторным управлением*, Tallinn Technical University, 2005. с56
- [IQM02] IQmath Library, *Module user's Guide, C28x Foundation Software*, Texas Instruments Inc., June 2002
- [DIG02] C28x Digital Motor Control Library, *Module user's Guide, C28x Foundation Software*, Texas Instruments Inc., June 2002
- [VIS04] *Visual C++ 6.0, Краткий обзор*, [http://www.interface.ru/fset.asp?Url=/microsoft/micro\\_dev.htm](http://www.interface.ru/fset.asp?Url=/microsoft/micro_dev.htm), INTERFACE Ltd. 2004

- [MAT04] *Matlab* 6.0, *Simulink*,  
<http://www.matlab.ru/simulink/default.asp>, The MathWorks, Inc. 2004
- [АНОХ01] В. Анохин, А. Ланнэ *MATLAB для DSP. Часть 1. Моделирование аналого-цифрового преобразования* 2001, Chip News, 2001
- [LEON00] Leonhard, Werner, *Regelung Elektrischer Antriebe*, Springer-Verlag GmbH, ISBN: 9783540671794, 462 Seiten, 2000
- [ГЕР01] Герман-Галкин С.Г. *Компьютерное моделирование полупроводниковых систем в МАТЛАБ 6.0: Учебное пособие.* – СПб.: КОРОНА принт, 2001. 320 с.
- [SIMU13] Matlab R13 Help, :Simulink.
- [ТИХ02] Тихомиров Д. *Анализ возможностей модернизации тягового привода трамвая КТ-4.* Работа бакалавра. – Таллинн: ТТУ институт электропривода и силовой электроники, 2002. – 48 с.
- [СТРО06] Строганов В.И. *Комбинированная энергоустановка городского автобуса с буферным источником мощности.* – Москва: Московский автомобильно дорожный институт, 2006. – 21 с.
- [КРАС06] Красулин А.С. Конспект лекций по дисциплине «*Эксплуатационные свойства транспортных средств*». – Украина: Приазовский государственный технический университет, 2006 – 62с
- [НА399] Олег Назаров, *Электропоезда ЭР2Р, ЭР2Т*  
<http://emupages.narod.ru/datasheet/er2r.htm>, 1999
- [КРУГ05] Энциклопедия Кругосвет®,  
<http://www.krugosvet.ru/articles/12/1001219/print.htm>, 2005
- [ЇKD06] Продукция/Тяговые двигатели,  
<http://www.pragoimex.cz/i/File/tam-1003-ru.pdf>, ЇKD PRAGOIMEX, 2006
- [SLOV06] Продукция/Тяговые двигатели,  
[http://www.slovres.sk/atr\\_t.htm](http://www.slovres.sk/atr_t.htm), SLOVRES a.s., 2006
- [ЇKOD06] Продукция/Тяговые двигатели,  
<http://www.skoda.cz/en/skoda-holding/products/c31702/drive-motor-ml-3336-k-4-aid774.html>, SKODA ELECTRIC a.s., 2006
- [EVER06] Продукция/Тяговые двигатели,  
<http://www.eversontesla.com/projects/proj2.html>, Everson Tesla Incorporated, 2006
- [КЛЮЧ80] В.И.Ключев, В.М.Терехов; *Электропривод и автоматизация общепромышленных механизмов*, М.: Энергия, 1980, 360 с.

- [КЕВ96] КЕВ AntriebsTehnik , "*Drives Application* ", номер 12, 1996 год.
- [IEC60349] IEC60349 – 2, <http://www.iec.cn>
- [ТЕХП05] Каталог продукции, *Тормозные резисторы для преобразователей частоты*. [http://www.tehprivod.ru/katalog/tor\\_rez.htm](http://www.tehprivod.ru/katalog/tor_rez.htm), 2005
- [БУЛ82] А.А.Булгаков; *Частотное управление асинхронными двигателями*, М.: Энергоиздат, 1982, 216 с.
- [LAUG94] J.Laugis, T.Lehtla; *Asünkroonajamite sagedusjuhtimine, Tallinna Tehnikaülikooli Elektrialamite ja jõuelektroonika instituut*, 1994, 91lk..
- [NASH97] J.Nash; Direct Torque Control, Induction Motor Vector Control Without an Encoder, IEEE Transactions on Industry Applications, vol.33, No. 2, March/April 1997
- [PENA02] Pena-Eguiluz R., Pietrzak-David M., Bernard de Fronel: *Comparison of Several Control Strategies for Parallel Connected Dual Induction Motors*, EPE-PEMC 2002, Dubrovnik & Cavtat, 2002.
- [MATS01] Y.Matsumoto, S.Ozaki, A.Kawamura; *A Novel Parallel – Connected Multiple Induction Motors Vector Control Method for the Rolling Stock Traction System*. IEE Transactions of Japan., 2001
- [MATR13] Matlab R13 Help.: SimPowerSystems.
- [FOC98] *Field Orientated Control of 3-Phase AC-Motors*, Literature number: BPRA073, Texas Instruments Europe, February 1998.
- [AHME97] Ahmet M., Hava y Seung-Ki Sul, Russel J., Kerkman z Thomas, A. Lipoу.: *Dynamic Overmodulation Characteristics of TriangleIntersection PWM Methods*, IEEE Industry Applications Society Annual Meeting New Orleans, Louisiana, October 5-9, 1997.
- [КУ302] Кузнецов С., *Моделирование тягового привода с векторным управлением*, Tallinn Technical University, 2002.
- [ЛАСК03] Б. ЛАСКА, Развитие тяговых преобразователей на транзисторах IGBT, Журнал "Железные дороги мира", номер 11, 2003
- [SEMI04]. SEMIKRON "*IGBT- application manual* ", 2004
- [LEO01] W.Leonhard; "Control of Elektrical Drives", Springer – Verlag, Berlin, 2001, 460 p.
- [ШРЕ00] Р.Т.Шрейнер; Математическое моделирование электроприводов переменного тока с полупроводниковыми преобразователями частоты, Е.: АООТ "Полиграфист", 2000.

- [МОН95] N.Mohan, T.M.Undeland, W.P.Robbins; "Power Electronics: Converters Application and Design", John Wiley & Sons, New York, 1995, 802 p.
- [САРБ80] Тиристорные преобразователи частоты в электроприводе. Под ред. Р.С. Сарбатова, М.: Энергия, 1980, 328 с.
- [РУД80] В.С. Руденко, В.И. Сенько, И.М. Чиженко; Основы преобразовательной техники, М.: Энергия, 1980, 424 с.
- [ШЁН85] Р. Шёнфельд, Э. Хабигер; Автоматизированные электроприводы. Пер. с нем, под ред. Ю. А. Борцова; Л.: Энергоатомиздат, 1985, 464 с.
- [СЕМ01] Б. Ю. Семёнов. Силовая электроника для любителей и профессионалов. – Москва: СОЛОН-Р, 2001. – 336 с.
- [КОП88] Справочник по электрическим машинам, Том 1, Москва, Энергоатомиздат, под редакцией И.П.Копылова, 1988
- [ШЁНФ85] Р. Шёнфельд, Э. Хабигер; Автоматизированные электроприводы. Пер. с нем, под ред. Ю. А. Борцова; Л.: Энергоатомиздат, 1985, 464 с
- [MOR97] J. Moreno-Eguílaz, Miguel Cipolla, Juan Peracaula "Induction Motor Optimum Flux Search Algorithms with Transient State Loss Minimization using a Fuzzy Logic based Supervisor", Polytechnic University of Catalonia, 1997.
- [BON00] Bon-Ho Bae, Seung-Ki Sul, Sang-Hoon Kim, Il-Ho Lee and Sung-Soo Han , " Application of Vector Control to Railway Vehicle " , Proceedings of the 2000 IPEC-TOKYO , 2000.
- [ТЕР87] В. М. Терехов, Элементы автоматизированного электропривода, Энергоатомиздат , Москва. 1987
- [БОЙ04] Виталий Бойко, *Макет привода с векторным управлением*, Topical Problems of Education in the Field of Electrical and Power Engineering“, Tallinn Technical University, 2004
- [TIEV02] Texas Instrument, TMS320F28x Event Manager (EV) Peripheral Reference Guide, Literature Number: SPRU065., 2002
- [SEU00] Seung-Ho Song, Jong-Woo Choi, Seung-Ki Sul: *Current measurements in digitally controlled AC drives*, Industry Applications Magazine, IEEE, Volume: 6 , Issue: 4 , Pages: 51 – 62, July-Aug 2000
- [BAR01] Bardos, P.: *Predicting the EMC performance of high frequency inverters*, Applied Power Electronics Conference and Exposition, 2001. APEC 2001. Sixteenth Annual IEEE, Volume: 1, Pages: 213 - 219 vol.1, 4-8 March 2001

- [NORM04] Norman J.: *New EMI Shielding Approaches*  
*Optimize Wireless Designs*, Chomerics, a division of Parker  
Hannifin Corp. Woburn, MA, 2004
- [HILL04] Hills P.: *EMC – Electromagnetic compatibility*,  
<http://homepages.which.net/~paul.hills/Emc/Emc.html>, Version 3.01, 22 Jun  
04
- [FRAN01] Francis J.: *AC Drives and EMI/RFI Mitigation*,  
[http://www.powerqualityanddrives.com/emi\\_rfi](http://www.powerqualityanddrives.com/emi_rfi), 2001
- [BONN02] Bonnie Baker C.: *Anti-Aliasing, Analog Filters for Data  
Acquisition Systems*, Microchip Technology Inc., 18 January 2002

## **ABSTRACT**

Work has been devoted to development of a new traction motor drive of municipal electric transport, predominantly trams and electric trains, on the basis of asynchronous engines with a short-circuited rotor. Work is devoted to the decision of the scientific problems related to improving existing and creation of new multimotor electric drives of an alternating current leading to an increase of the transport productivity and reliability and to improve its technical, economic, and ergonomic odds.

Thematic topicality is explained by the practical needs of the country in effective, ergonomic, and safe transport means. Research is based on the novel theoretical results and progressive technologies in the field of driving engineering and power electronics, developed in last years in the European Union and particularly in Estonia.

The new concept of a drive will allow to reduce expenses for maintenance service essentially. Application of algorithms of vector management by a drive will allow receiving greater starting moments and high smoothness of a course. The developed concept of a drive with small completions can be used on any rail transport. Application of this drive in Estonia is possible on the Estonian electric railway and in development of trams.

Work consists of 4 chapters. The first chapter is devoted to research and classification of decisions of an electric traction drive available in the world for railway transport. The second chapter is devoted to development and approbation of the novel method of structural and power TAMD synthesis. In the third chapter building the method of the TAMD frequency converter design is described. In the final chapter computer modelling and an experimental research of components of the electric drive are investigated.

## LÜHIKOKKUVÕTE (ANNOTATSIOON)

Dissertatsioon käsitleb raudteetranspordi, peamiselt trammide ja elektrirongide jaoks uute veoajamite uurimist ja väljatöötamist. Töö eesmärgiks on mitme asünkroonmootoriga veoajami uute tehniliste ja tarkvaraliste lahenduste loomine. Lahendatud on mitme asünkroonmootoriga veoajamitega seotud teaduslikud probleemid eesmärgiga tõsta elektritranspordi tõhusust ja töökindlust, samuti parandada nende tehnilisi, majanduslikke ning ergonoomilisi omadusi.

Töö teema on aktuaalne seoses efektiivse, ergonoomilise ning ohutu ühistranspordi arendamisega.

Uuringud on tehtud uute teoreetiliste tulemuste ja moodsa tehnoloogia baasil elektriajamite ja jõuelektronika valdkonnas, mida on viimastel aastatel arendatud nii Euroliidus kui ka Eestis.

Veojami uus kontseptsioon aitab oluliselt vähendada tehnilise hoolde kulusid. Uute vektorjuhtimise algoritmide kasutuselevõtt tagab suure käivitusmomendi ja sujuva sõidu. Loodud kontseptsiooni saab väikeste kohandustega kasutada mis tahes rööbastranspordivahendil, Eestis nii Elektriraudteel kui ka Tallinna trammide arendamisel.

Doktoritöö koosneb neljast peatükist. Esimeses uuritakse ja klassifitseeritakse olemasolevate elektri-veojamite lahendusi raudteetranspordi valdkonnas. Teises vaadeldakse veoajami struktuuri, lülitus- ja juhtimissüsteemide sünteesi. Kolmandas peatükis kirjeldatakse sagedusmuundurite projekteerimismetoodikat. Viimases peatükis uuritakse teoreetiliselt ja eksperimentaalselt erinevate arvutimudelite kasutusvõimalusi ning ajamikomponentide tööd.

## PUBLICATION

1. Vitali Boiko *Vibrationsmeßgerät auf der Basis von Signalprozessor*. Actual Problems of Electrical Drives And Industry Automation, Estonia: Tallinn, 1999.
2. Juhan Laugis, Dmitri Vinnikov, Vitali Boiko *Analysis of drawbacks and reconstruction problems of the R2-type train*. BEC'2000: 7<sup>th</sup> Biennial Conference on Electronics and Microsystem Technology, October 8-11, Tallinn Tech. University, 2000.
3. Vitali Boiko *Electromechanical Voltage Converters in Electric Transport of Estonia*. The 3rd Research Symposium of Young Scientists: Actual Problems of Electrical Drives and Industry Automation, Tallinn Tech. University, Tallinn, May 19 - 26, 2001, pp. 74-75.
4. Ю. Лаугис, Т. Лехтла, Ю. Йоллер, В. Бойко, Д. Винников, М. Лехтла *Состояние и тенденции развития электротранспорта Эстонии*. III Международная конференция по автоматизированному электроприводу (АЭП-2001), Нижний Новгород, 12 - 14 сентября 2001 года.
5. В. Бойко, Д. Винников, Ю. Лаугис, С. Игнатов *Модернизация установки "Universalprüfmaschine Zwick 1435" на Пярнуской лыжной фабрике*. Automation and control technologies, Kaunas, 2002.
6. Boiko, V., Vinnikov, D., Liivik, L. *Automotive applications of ultracapacitors*. Summer Seminar on Nordic Network for Multi Disciplinary Optimised Electric Drives. Taipalsaari, Finland, June 15-17, 2002.
7. Д. Винников, В. Бойко, Ю. Лаугис *Разработка и исследование статического преобразователя напряжения для трамвая*. Силовая электроника и энергоэффективность сээ'2002, Ukraine, 2002.
8. J. Laugis, T. Lehtla, J.Joller, V.Boiko, D. Vinnikov, M.Lehtla *Modernization of electrical transport systems in Estonia*, 10-th International POWER ELECTRONICS and MOTION CONTROL Conference EPE-PEMC, Cavtat & Dubrovnik, 2002.
9. Boiko, V., Vinnikov, D., Joller, J. *Use of Ultracapacitors Modules in ICE Starting System*. Power and Electrical Engineering International Scientific Conferenc, Riga, Latvia, October 10-14, 2002.
10. Vitali Boiko *Comparison of possible drive control methods for electrical rail vehicle*. The 4<sup>th</sup> Research Symposium of Young Scientists, Actual Problems of electrical drives and industry automation, Tallinn, Estonia, May 17-21, 2003 .

11. Vitali Boiko, Juhan Laugis *Comparison of possible ac drive control methods for kt4 tram*. 3rd International Workshop CPE 2003, Compatibility in Power Electronics, Gdańsk - Zielona Góra, POLAND, May 28-30, 2003.
12. Vitali Boiko, Dmitri Vinnikov, Juhan Laugis *Анализ возможности замены автомобильной аккумуляторной батареи на ультраконденсатор*. Международная научно-техническая конференция “11 Бернардовские чтения”, Иваново, Российская Федерация, 4-6 июня, 2003.
13. Д. Винников, В. Бойко, Ю. Лаугис *Исследование возможностей применения ультраконденсаторов в электросистеме автомобиля*. Технічна електродинаміка, Ukraine, Kiiev, 2003.
14. Vitali Boiko, Dmitri Vinnikov *Eesti elektriraudtee kontaktvõrgu seisund ja valjavaated*. ELEKTRIALA Nr.1, 2004.
15. Vitali Boiko, *Макет привода с векторным управлением*. Topical problems of education in the field of electrical and power engineering, Kuressaare, Estonia, January 19 - 24, 2004.
16. В. Бойко, Д. Винников, Ю. Лаугис *Решение задачи измерения скорости в макете привода с векторным управлением*. Automation and Control Technology, Kaunas, 2004.
17. Dmitri Vinnikov, Vitali Boiko *Development of the Dual-Output Auxiliary Power Supply*. Summer Seminar on Nordic Network for Multi Disciplinary Optimised Electric Drives, Tallin, Estonia, June 4-6, 2004.
18. V. Boiko, J. Laugis *Behavior of the Dual-Motor Traction Drives in the Different Operation Modes*. 11<sup>th</sup> International Power Electronics and Motion Control Conference, Riga, Latvia, September 2-4, 2004.
19. Vitali Boiko, Juhan Laugis *Моделирование динамического ослабления поля асинхронного двигателя*, Технічна Електродинаміка, 2004, ISSN 0204-3599.
20. Д. Винников, В. Бойко, М. Лехтла, А. Росин, Ю. Лаугис *Об опыте института электропривода и силовой электроники ТТУ в области модернизации электроподвижного состава Таллинского трамвайного парка*. Технічна електродинаміка, Ukraine, Kiiev, 2004, ISSN 0204-3599.
21. V. Boiko, J. Laugis *A Speed Measurement Method In The Model Drive With Field-Oriented Control*. Proceedings of the 9th Biennial Baltic Electronics Conference, Tallinn University of Technology, October 3-6, 2004 Tallinn, Estonia.

22. Thomas Kimmer, Vitali Boiko, Juhan Laugis *Bestimmung der Parameter des Ersatzschaltbildes eines Asynchronmotors für eine feldorientierte Regelung*. 2nd International Symposium „Topical Problems of Education in the Field of Electrical and Power Engineering“ Tallinn University of Technology, January 17 – 22, 2005, ISBN 9985-69-033-8, p98.
23. Vitali Boiko, Dmitri Vinnikov *Elektrirongide ER1 ja ER2 veojami energiavoogude analüüs*. ELEKTRIALA Nr.1, 2005.
24. Dmitri Vinnikov, Vitali Boiko *TTÜ elektriajamite ja jõuelektroonika instituut moderniseeris BLRT kraana*. Mente at Manu , May 5, 2005.
25. В. Бойко, Д. Винников *Об опыте проведения курсов повышения квалификации в институте электропривода и силовой электроники Таллиннского Технического Университета*. Automation and control technologies – 2005, p 15-17, 2005, ISBN 9955-09-864-3.
26. V. Boiko, J. Laugis *EMI problems of current measurements in inverters with high switching frequency*. Proceedings of 4th International Workshop CPE 2005 Compatibility in Power Electronics, 135-137, June 1-3, 2005, ISBN 83-7421-075-3.

## ELULOOKIRJELDUS

### 1. Isikuandmed

Ees- ja perekonnanimi Vitali Boiko  
 Sünniaeg ja -koht 21.09.1975, Turov, Valgevene  
 Kodakondsus Eesti

### 2. Kontaktandmed

Aadress Metsa 10, 76401, Laagri, Eesti  
 Telefon (+372) 56801959  
 E-posti aadress vitali\_b@hotmail.com

### 3. Hariduskäik

Õppeasutus (nimetus lõpetamise ajal)	Lõpetamise aeg	Haridus (eriala/kraad)
Tallinna Tehnikaülikool	1999	Tehnikateaduste magistrikraad
Tallinna Tehnikaülikool	1997	Inseneri diplom(energiatehnika)
Pärnu 3. Keskkool	1992	keskharidus
Pärnu 7. Põhikool	1990	põhiharidus

### 4. Keelteoskus (alg-, kesk- või kõrgtase)

Keel	Tase
Vene	Kõrgtase
Eesti	Keskase
Saksa	Keskase

Inglise	Kesktaase
---------	-----------

#### 5. Täiendusõpe

Õppimise aeg	Täiendusõppe läbiviija nimetus

#### 6. Teenistuskäik

Töötamise aeg	Tööandja nimetus	Ametikoht
2005-	ABB AS	müügijuht
2001-	TTÜ	teadur
1998-2001	IDL, Rostock, Saksamaa	programmeerija

#### 7. Teadustegevus

2001 130L "Elektriraudtee kontaktvõrgu ja veolajaamade tehnilise seisundi uuring – lepinguline teadus- ja arendustöö "

2002 202L "Trammide elektriajamite ja jõumuundurite moderniseerimine"

1999-2001 T222 "Energiasäästlike elektriajamite väljatöötamine ja rakendamine Eesti energeetikas, tööstuses ja transpordis"

2001 G 4852 "Elektriajamite ja jõupooljuhtmuunduri parameetrite diagnostika talitluse tõhustamiseks ja töökindluse suurendamiseks"

#### 8. Kaitstud lõputööd

Magistritöö "Vibratsioonitaseme mõõtmise seade signaalprotsessori ADSP baasil", TTÜ, 1999

Diplomitöö "Pöördlaua maketi programmjuhtimine" ,TTÜ, 1997

#### 9. Teadustöö põhisuunad

Jõupooljuhtmuundurite, ajamite ja ajamitel põhineva tehnoloogia energiavoo juhtimine, energiamuundusprotsessid, ajamid ja nende juhtimistarkvara, elektersõidukite veoajamid ja mundurid.

#### 10. Teised uurimisprojektid

2001-2002 105L "Trammide veoajamite rekonstrueerimine"

2000 4/011L “Elektriveduri ER2 peaveoajami tehnilis-  
majanduslike näitajate analüüs ja ettepanekud moderniseerimiseks”

## CURRICULUM VITAE

### 1. Personal data

Name Vitali Boko  
Date and place of birth 09.21.1975, Turov, Belarussia

### 2. Contact information

Address Metsa 10, 76401, Laagri, Eesti  
Phone (+372) 56801959  
E-mail vitali\_b@hotmail.com

### 3. Education

Educational institution	Graduation year	Education (field of study/degree)
Tallinn University of Technology	1999	Master of Science in Technology (Electrical Drives and Power Electronics)
Tallinn University of Technology	1997	Diploma ingeneer (Energy Technology)
Pärnu Secondary School No. 3	1992	Secondary Education
Pärnu Basic School No. 7	1990	Basic Education

### 4. Language competence/skills (fluent; average, basic skills)

Language	Level
English	Middle
Russian	High

Estonian	Middle
German	Middle

#### 5. Special Courses

Period	Educational or other organisation

#### 6. Professional Employment

Period	Organisation	Position
2005-	ABB AS	Sales manager
2001-	TUT	Researcher
1998-2001	IDL, Rostock, Germany	Programmer

#### 7. Scientific work

2001 130L "Research of technical status of traction substations and contact networks of Estonian electric railway"

2002 202L "Modernization of tram electrical drives and power converters".

1999-2001 T222 "Designing of energy saving electrical drives for Estonian power engineering, industry and transport"

2001 G 4852 "Diagnostics of electrical drives and power electronic converters for improvement of operation and reliability"

#### 8. Defended theses

"Vibration measurement device on the DSP basis", (TUT, 1999, M. Sc.)

"Programming of the model of a boring machine" ,(TUT, 1997, Dipl. Eng.)

#### 9. Main areas of scientific work/Current research topics

Control of energy flows in drives and in drive-based technology, energy exchange processes, software based control of drives, traction drives and converters of electric vehicles.

10. Other research projects

2000 “The technical and economic research of the R2-type train traction drive”

2001-2002 105L “Reconstruction of tram traction drives”